

Published in final edited form as:

ChemMedChem. 2009 October ; 4(10): 1615–1629. doi:10.1002/cmdc.200900226.

2,3-Dihydro-1-Benzofuran Derivatives as a Series of Potent Selective Cannabinoid Receptor 2 Agonists: Design, Synthesis, and Binding Mode Prediction through Ligand-Steered Modeling

Dr. Philippe Diaz^[a], Sharangdhar S. Phatak^[b], Dr. Jijun Xu^[c], Frank R. Fronczek^[d], Fanny Astruc-Diaz^[a], Prof. Charles M. Thompson^[a], Prof. Claudio N. Cavasotto^[b], and Prof. Mohamed Naguib^[c]

Mohamed Naguib: Naguib@mdanderson.org

^[a]Core Laboratory for Neuromolecular Production, Department of Biomedical and Pharmaceutical Sciences, The University of Montana, 32 Campus Drive, Missoula, MT 59812 (USA)

^[b]School of Health Information Sciences, The University of Texas Health Science Center at Houston 7000 Fannin, Suite 860B, Houston, TX 77030 (USA)

^[c]Department of Anesthesiology and Pain Medicine, The University of Texas M. D. Anderson Cancer Center, Houston, TX 77030 (USA), Fax: (+1) 713-792-7591

^[d]Chemistry Department, Louisiana State University, Baton Rouge, LA 70803-1800 (USA)

Abstract

We recently discovered and reported a series of *N*-alkyl-isatin acylhydrazone derivatives that are potent cannabinoid receptor 2 (CB₂) agonists. In an effort to improve the druglike properties of these compounds and to better understand and improve the treatment of neuropathic pain, we designed and synthesized a new series of 2,3-dihydro-1-benzofuran derivatives bearing an asymmetric carbon atom that behave as potent selective CB₂ agonists. We used a multidisciplinary medicinal chemistry approach with binding mode prediction through ligand-steered modeling. Enantiomer separation and configuration assignment were carried out for the racemic mixture for the most selective compound, MDA7 (compound **18**). It appeared that the *S* enantiomer, compound MDA104 (compound **33**), was the active enantiomer. Compounds MDA42 (compound **19**) and MDA39 (compound **30**) were the most potent at CB₂. MDA42 was tested in a model of neuropathic pain and exhibited activity in the same range as that of MDA7. Preliminary ADMET studies for MDA7 were performed and did not reveal any problems.

Keywords

agonists; benzofuran derivatives; cannabinoid receptor 2; ligand-steered modeling; receptors

Introduction

The endogenous cannabinoid system is a complex system consisting of two cannabinoid receptors (cannabinoid receptors 1 [CB₁] and 2 [CB₂]), seven endogenous (endocannabinoid) ligands,^[1] and several proteins responsible for the regulation of

endocannabinoid metabolic pathways, such as monoacylglycerol lipase and fatty acid amide hydrolase.^[2] Modulation of this system has significant consequences in terms of immunomodulation. CB₂ stimulation suppresses microglial cell activation and neuroinflammation,^[3, 4] which may explain why CB₂ is an emergent target for the treatment of neuropathic pain.^[5–8] On the other hand, use of CB₂ inverse agonists has been studied for the treatment of allergic contact dermatitis in animal models.^[9] Increases in endocannabinoid concentrations seem to be a protective mechanism aimed at counteracting pain and inflammation.^[10]

The two cannabinoid receptors that have been characterized and cloned, CB₁ and CB₂,^[11, 12] have significant differences in terms of localization and function. CB₁ is found predominantly in the brain^[13] and is linked to cognitive impairment and psychoactivity.^[14] These adverse effects preclude the development and use of CB₁ agonists as therapeutics. CB₂ is expressed mainly on immune tissues—the spleen, tonsils, monocytes, and B and T lymphocytes.^[12, 15] CB₂ mRNA and/or protein levels are increased during different inflammatory conditions.^[3, 4] Modulation of CB₂ appears not to cause central side effects.^[6, 7]

Neuropathic pain is caused by lesions in the central or peripheral nervous system and is characterized by hyperalgesia, reduced nociceptive thresholds such that normally innocuous stimuli cause pain, and allodynia (touch-evoked pain). Neuropathic pain is triggered by conditions such as diabetic neuropathy, AIDS-related neuropathy, postherpetic neuralgia, degenerative spinal disease, chemotherapy, radiotherapy, complex regional pain syndrome, phantom limb pain, trigeminal neuralgia, and multiple sclerosis. Neuropathic pain is refractory to traditional analgesics. The current typical treatments for neuropathic pain—opioids, gabapentin, and amitriptyline—are effective in fewer than 30 % of patients.^[16–20] Neuropathic pain negatively affects patients' physical, emotional, and social quality of life.^[21] Recently, however, CB₂ has emerged as a new target for the treatment of neuropathic pain.^[7, 8, 22–24] Upregulation of CB₂ mRNA and proteins in the dorsal root ganglia and spinal cord is also found in animals after spinal nerve ligation^[23, 25] or nerve injury.^[26–28]

Recently, the potential utility of CB₂ agonists as treatments for neuropathic pain has received much attention. Several CB₂ selective agonists have been described,^[5, 6, 29–37] and in the last 2 years, more than 150 patents have been granted on CB₂ modulators.

Some of these compounds (Figure 1) have been widely used in in vivo animal models of neuropathic pain. Compound **1** better drug-like profile. A novel series based on a 3,3-disubstituted-2,3-dihydro-1-benzofuran ring was designed to increase bioavailability compared with the isatin series. On the basis of a comparison of the benzofuran and isatin structures, we assumed that the benzofuran scaffold might mimic the isatin scaffold (Figure 2). In Figure 2, ring B in the benzofuran series is superimposable with ring B in the isatin series formed by the hydrazone and the indolone through an internal hydrogen bond. In this case, the two five-membered rings (ring A) from the benzofuran and isatin structures fit. The absence of ring C in the benzofuran series is expected to decrease lipophilicity of the benzofuran series compared with the isatin series. This benzofuran series was synthesized using a colloidal palladium nano-particle-catalyzed tandem cyclization/cross-coupling reaction. We previously described the detailed pharmacological profile of one of these benzofuran compounds, compound **18**.^[7] This compound reversed neuropathic pain in spinal nerve ligation and paclitaxel-induced neuropathy models in rats without affecting locomotor behavior, and the effects of this compound were selectively antagonized by a CB₂ receptor antagonist but not a CB₁ receptor antagonist.^[7] In this report, we describe the design, synthesis, and structure-activity (Figure 1) has been described as a protean

agonist.^[38,39] Compound **2**, a well-characterized selective CB₂ agonist, showed efficacy in models of inflammatory, postoperative, neuropathic, and osteoarthritic pain.^[6] Compound **3** was chosen as a clinical candidate for the treatment of inflammatory pain.^[30] Recently, the pharmacokinetics and safety in humans of compound **4**, a nonselective CB₁/CB₂ agonist with limited brain penetration acting on the peripheral nervous system,^[40] have been reported on the basis of results of phase I studies.^[41] We recently described compound **5**, which has a profile similar to that of compound **4** and which showed potent antiallodynic effects in a rat model of neuropathic pain but did not affect rat locomotor activity.^[42] Systemic administration or intrathecal administration of compound **6**^[43] reduced both evoked and spontaneous wide-dynamic-range neuronal activity in neuropathic but not sham-treated rats. The effects in neuropathic rats were blocked by pre-administration of a CB₂, but not a CB₁, receptor antagonist.^[44]

We recently described a series of *N*-alkyl isatin acylhydrazone derivatives that are potent CB₂-selective agonists^[42] and a series of CB₂-selective inverse agonists.^[45] The agonists suffer from poor water solubility, and in our efforts to better understand and improve the treatment of neuropathic pain, we sought to design and synthesize a series of agonists with a relationships (SARs) of this series of benzofuran compounds and the biological activities of both enantiomers of compound **18**. Structural modeling studies based on ligand-steered modeling of the agonist: CB₂ complex binding site are also presented, supporting a structural rationalization of SAR data.

Methods

Chemistry

The syntheses are outlined in Schemes 1–3. Compounds **10 a** (Scheme 1) and **10 b** (Scheme 2) were obtained from the corresponding phenols^[46,47] by coupling with 3-bromo-2-methylpropene using potassium carbonate in methyl ethyl ketone. The resulting ethers were submitted to a palladium-catalyzed tandem cyclization/Suzuki-coupling reaction to afford benzofuran **11 a**, **11 b**, and **11 c**.^[48,49] After saponification, the resulting carboxylic acids (**12 a** to **12 c**) were coupled with amines using HATU, DiPEA to afford compounds **13** and **14** and **16** to **24**. To study the impact of substitution at carbone 3, the palladium-catalyzed tandem cyclization/Suzuki-coupling reaction was done in the last step (Scheme 3). Carboxylic acid **25** was obtained from **10 b** by saponification using sodium hydroxide. Then, **25** was coupled with cyclohexylamine or piperidine using HATU, DiPEA to afford compounds **26 a** and **26 b**. Compounds **26 a** and **26 b** were submitted to palladium-catalyzed tandem cyclization/Suzuki-coupling reaction to afford compounds respectively **27** and compounds **28** to **32**. This synthetic pathway (Scheme 3) was not used for compounds **19** and **20**, as their retention factors were close to the retention factors of, respectively, compounds **26 b** and **26 a**.

Enantiomeric separation

Seven hundred fifty milligrams of the racemic mixture of compound **18** was processed using a Cyclobond DMP column and a mixture of acetonitrile, acetic acid, and triethylamine as mobile phase at a temperature of 10°C. Purity analysis indicated that compound **33** has an enantiomeric purity of 97.3 % while compound **34** has an enantiomeric purity of 97.5 %.

Crystallographic analysis and assignment of absolute configuration

The structure of compound **33** was confirmed by X-ray diffraction. Compound **33** yielded crystals of suitable quality for X-ray diffraction by slow evaporation of an ethyl acetate/heptane solution (Figure 3). The crystal structure was determined using X-ray data collected at 90 K, with Cu K α radiation ($\lambda=1.54178$ Å) on a Bruker Kappa Apex-II diffractometer.

Crystals are mono-clinic, space group $P2_1$ with $Z = 2$. All H atoms were visible in difference maps and were placed in calculated positions in the refinement, with a torsional parameter refined for the methyl group, leading to $R = 0.029$, $R_w = 0.075$ for 228 refined parameters and 3026 independent reflections having $\theta_{\max} = 68.8^\circ$. The absolute configuration was determined, on the basis of resonant scattering from light atoms only, to be (S) at C14, using 1266 Bijvoet pairs. The Flack parameter^[50] has a value of $x = 0.07(19)$, and the Hooft parameter^[51] has a value of $y = 0.03(8)$, corresponding to a probability of 1.000 that the reported absolute configuration is correct. The CIF has been deposited at the Cambridge Crystallographic Data Centre, CCDC 725803.

Ligand-steered modeling of the agonist: CB₂ complex binding site

It should be emphasized that there is no crystal structure of an active-state class-A G-protein-coupled receptor (GPCR). Thus, structural modeling studies were performed on the benzofuran derivatives to identify a putative binding mode of this class of CB₂ agonists. The crude homology model of the active-state CB₂ receptor developed in this study was based on a multitemplate approach^[52–54] using (1) the recently described crystallized structures of the β_2 -adrenergic and ligand-free opsin class-A GPCRs, to take advantage of several features of the purported active state of class-A GPCRs that are not completely present in either crystal structure, and (2) the information obtained from several computational studies that have proposed the active state models of CB₂ and other class-A GPCRs.^[55–65]

The CB₂, β_2 -adrenergic (PDB code 2RH1), and ligand-free opsin (PDB code 3CAP) sequences were aligned on the basis of existing information on conserved residues within class-A GPCRs.^[66] CB₂ lacks the conserved proline in helix 5, so the next highly conserved residue, tyrosine, was used for the alignment as described by Xie et al.^[67] The nomenclature of Ballesteros, Weinstein, and Stuart is used, whereby the most conserved residue in helix X is labeled X.50.^[68] The resulting sequence alignment was used as an input to MODELLER 9v4^[69] to develop a crude CB₂ model. The N- and C-terminus residues (amino acids 1–26 and 316–360) of CB₂, the T4 L residues connecting helix 5 and 6 of β_2 , helices 5–7 of β_2 , and helices 1–4 of ligand-free opsin were omitted. Mutagenesis and other CB₂ modeling studies suggest the possibility of a disulfide bond between residues Cys 174 and Cys 179 in the E2-loop, which was included in our homology model.^[70,71] On the basis of information in the literature,^[62] helix 3 of CB₂ was rotated counterclockwise (as seen from the extracellular side) using the GPCR Helix Manipulator script available under Maestro from Schrödinger LLC.^[72] This was followed by a restraint-minimization procedure to relieve the structural strain stemming from the replacement of nonconserved residues in the homology modeling process while the pocket was kept intact.

The ligand-steered modeling method has already been described in full.^[45,73, 74] Briefly, starting from the crude model developed through a multitemplate approach, a known agonist was seeded into the pocket, and a structural ensemble of 200 structures was generated by randomizing the position and orientation of the ligand, followed by a multistep energy minimization in which the van der Waals interaction was gradually switched from soft to full interaction, as performed in other cases.^[73, 75–77] The ligand and receptor were held flexible in this stage without any restraints. The structures in the ensemble were ranked using crude binding energy estimation, and then 40 structures were subjected to a full flexible-ligand-flexible-side chain Monte Carlo-based global energy optimization. The top-ranking structures were then visually inspected for ligand:receptor interactions, and complex candidates were selected.

Pharmacology

Cannabinoid-receptor-mediated functional activity—Functional activity was evaluated using γ -[³⁵S]GTP assays in Chinese hamster ovarian cell membrane extracts expressing recombinant human CB₁ (hCB₁) or human CB₂ (hCB₂). The assay relies on the binding of γ -[³⁵S]GTP a radiolabeled nonhydrolyzable GTP analogue, to the G protein upon binding of an agonist of the GPCR. In this system, agonists stimulate γ -[³⁵S]GTP binding, whereas antagonists have no effect and inverse agonists decrease γ -[³⁵S]GTP basal binding. CB₁ and CB₂ assay data are presented as the mean of two determinations. Assay reproducibility was monitored by the use of a reference compound, compound **7**. For replicate determinations, the maximum variability tolerated in the test was of $\pm 20\%$ around the average of the replicates. Efficacies (E_{\max}) for CB₁ and CB₂ are expressed as a percentage of the efficacy of compound **7**.

Binding assays—Compounds **18**, **19**, **20**, **29**, and **30** were screened in a competitive binding experiment using membranes of Chinese hamster ovarian K1 cells selectively expressing hCB₂ at different concentrations in duplicate.^[78] The competitive binding experiment was performed in 96-well plates (Masterblock) containing binding buffer (50 mM Tris, pH 7.4, 2.5 mM EDTA, 0.5 % protease-free bovine serum albumin), recombinant membrane extracts (0.25 μ g protein/well), and 1 nM [³H]**7** (PerkinElmer, NEX-1051, 161 Ci/mmol, diluted in binding buffer). Nonspecific binding was determined in the presence of 10 μ M compound **7** (Tocris Bioscience). The sample was incubated in a final volume of 0.1 mL for 60 min at 30°C and then filtered on a GF/B UniFilter microplate (PerkinElmer, catalogue number 6005177) pre-soaked in 0.5 % polyethyleneimine for 2 h at room temperature. Filters were washed six times with 4 mL of cold binding buffer (50 mM Tris, pH 7.4, 2.5 mM EDTA, 0.5 % protease-free bovine serum albumin), and the amount of bound [³H]**7** was determined by liquid scintillation counting. Median inhibitory concentration (IC₅₀) values were determined by nonlinear regression using the one-site competition equation. The inhibition constant (K_i) values were calculated using the Cheng-Prus-off equation ($K_i = IC_{50} / (1 + (L / K_D))$), where L = concentration of radioligand in the assay and K_D = affinity of the radioligand for the receptor.

In vivo evaluation

Animals—Adult male Sprague Dawley rats (Harlan Sprague Dawley) weighing 120–150 gm were used in experimental procedures approved by the Animal Care and Use Committee of The University of Texas M. D. Anderson Cancer Center. Animals were housed three per cage on a 12-hour-light/12-hour-dark cycle with water and food pellets available *ad libitum*.

Paclitaxel-induced neuropathy model—Groups of rats ($n = 5-7$) received either vehicle (10 % Cremophor EL in saline) or 1.0 mg kg⁻¹ of paclitaxel daily by intraperitoneal injection for 4 consecutive days for a final cumulative dose of 4 mg kg⁻¹;^[7, 79] the injection volume was 1 mL kg⁻¹. Baseline responses to mechanical stimulation of the hind paw (see next paragraph) were established on day 0 and continued daily until the development of neuropathy was confirmed.

Assessment of mechanical withdrawal thresholds—For assessment of antiallodynic effect, rats were placed in a compartment with a wire mesh bottom and allowed to acclimate for a minimum of 30 min before testing. Mechanical sensitivity was assessed using a series of Von Frey filaments with logarithmic incremental stiffness (0.41, 0.70, 1.20, 2.00, 3.63, 5.50, 8.50, and 15.1 g) (Stoelting, Wood Dale, IL), as previously described,^[80] and 50 % probability withdrawal thresholds were calculated with the up-down method.^[81] In brief, beginning with the 2.00 g probe, filaments were applied one by one to the plantar surface of a hind paw for 6–8 s. If no withdrawal response was observed, the next

stiffer filament was applied; if there was a withdrawal response, the next less stiff filament was applied. Six consecutive responses after the first change in the response were used to calculate the withdrawal threshold (in grams). When response thresholds fell outside the range of detection, 15.00 g was assigned for absence of response to all tested fibers, and 0.25 g was assigned for withdrawal response to all tested fibers. The percentage maximal possible effect was calculated as $([\text{postdrug threshold} - \text{baseline threshold}] / [\text{cutoff threshold} (15 \text{ g}) - \text{baseline threshold}]) \times 100$.

Data analysis

Statistical analyses were carried out using BMDP 2007 (Statistical Solutions, Saugus, MA). Data were analyzed using one-way analysis of variance (ANOVA) or *t* test, where appropriate. If findings on ANOVA were significant, Tukey–Kramer post hoc analysis was used for multiple group comparison. Area under the curve was calculated using the trapezoidal rule. The results are presented as mean \pm standard error of the mean and were considered significant at $P < 0.05$.

ADMET

Compound **18** was tested for the following: aqueous solubility (PBS, pH 7.4) at 2.0×10^{-4} M at a chromatographic wave length of detection of 230 nm,^[82] plasma protein binding with %recovery (human) at 1.0×10^{-5} M,^[83] A-B permeability at 1.0×10^{-5} M,^[84] and B-A permeability at 1.0×10^{-5} M,^[85] Ames test^[86] and automated whole-cell patch-clamp technique (Qpatch 16 by Sophion Biosciences) were used to record outward potassium currents (hERG) from single cells.^[87]

Results and Discussion

Ligand-steered modeling of the agonist–CB₂ complex

Because there is no published crystal structure of the active state of CB₂, we aimed to structurally characterize the agonist:CB₂ complex to identify residues involved in ligand recognition and thus explain SAR data for the benzofuran class of agonists. Recently, ligand-steered homology modeling, in which known ligands are explicitly used to shape and optimize the binding site through a docking-based stochastic global energy minimization procedure, was developed and tested in melanin-concentrating hormone receptor 1, a class-A GPCR target.^[73] The ligand and receptor are considered flexible throughout the modeling process, which ensures proper coverage of the interaction energy landscape. This method was recently successfully applied in two different applications in the drug discovery process: high-throughput docking-based discovery of novel chemotype inhibitors for melanin-concentrating hormone receptor 1^[73] and structural characterization of inverse agonists binding to CB₂.^[45] Ligand-steered modeling of the binding site is especially useful when there is only limited and inconclusive structural information available about protein:ligand interactions. To accomplish our aim, we implemented this methodology to build a multitemplate homology model of CB₂ in a putative agonist-bound conformation, based on available information about similar active-state models of class-A GPCRs^[58–61,63–65,88] and crystal structures of the β_2 -adrenergic^[55–57] and ligand-free opsin receptors.^[89]

Multi-template approach to develop an initial CB₂ homology model

It is well known that the quality and accuracy of homology models depends on the choice of the template protein structure and its sequence alignment with the target sequence.^[74,90,91] However, a single template structure may not represent a physiologically relevant conformation, and if this is the case, the result is an inaccurate homology model. The use of two or more homologous template structures, termed multitemplate homology modeling, has

recently been successfully used to improve the accuracy of structural models.^[52–54] In the case of CB₂ and other class-A GPCRs, rotational movement of helix 3 and/or helix 6, translational motion of helix 5 towards helix 6, and outward tilting of helix 6 coupled with structural changes, like breakage of “ionic lock” between R3.50 and D/E6.30 residues, seem to characterize the active state, thus complicating the modeling.^[58–65,88] Though the crystal structure of the ligand-free opsin^[89] explains the movements of helices 5 and 6 and the breakage of ionic lock relevant for agonist-induced conformations, it fails to explain the displacement of extracellular loop 2 away from the transmembrane core, as seen in the crystal structure of human β_2 -adrenergic receptor, which may play an important role in capturing diffusible ligands by providing the ligands access from the extracellular environment into the transmembrane core of GPCRs.^[64,89,92, 93] This displacement of extracellular loop 2 away from the transmembrane core is difficult to explain on the basis of the ligand-free structure of opsin. However, it should be noted that the β_2 -adrenergic receptor was crystallized with inverse agonist carazolol,^[55–57] hence, it may not be suited to model an active-state structure by itself. Therefore, considering that neither crystal structure is suitable as is to model an active-state GPCR, and on the basis of the experimental and modeling evidence reported above, we incorporated several features from both crystal structures (helices 1–4 and extracellular loop 2 from β_2 -adrenergic crystal structure, helices 5–7 from ligand-free opsin structure and manual rotation of helix 3), thus developing an initial multitemplate model of active-state CB₂. Thus, this initial model includes several well-known structural features of the agonist-bound conformations of class-A GPCRs as described earlier.

Structural characterization of the agonist-bound CB₂ binding site in agreement with experimental evidence

The current experimental and computational modeling studies indicate that hydrogen bonds, π - π stacking, and/or van der Waals interactions with residues of helices 3–7 account for most of the known ligand:CB₂ interactions.^[60,62, 72,94–97] Prior modeling, SAR, and mutagenesis studies have suggested the presence of an aromatic pocket within helices 3, 5–7 surrounded by residues Y5.39, F5.46, W5.43, and W6.48, and hydrogen-bond interactions with S3.31, T3.35, Y5.39, and N7.45.^[60,62, 94–98] Mutagenesis studies seem to indicate that interactions with S3.31 and F5.46 are crucial to improve selectivity as compared with CB₁.^[95] However, ligand:receptor interactions vary with ligand chemotypes, and there is no total agreement on the binding site and mode of CB₂ agonist compounds. From the set of compounds displaying CB₂ agonist activity (Table 1), we selected compound **33** to model the binding site with the ligand-steered method, analogous to what has been done with GPCRs and other receptors.^[45,73, 75,76,99–102] Because of the sensitivity of hCB₂ half-maximal effective concentration (EC₅₀) values (Table 1) to C3 substitutions, we hypothesized that the R1 group was facing towards the hydrophobic pocket located in the interior of the transmembrane domain. Hence, in our initial model, the R1 group was oriented towards that pocket. Given the similarities between the isatin scaffold and the benzofuran scaffold, it was assumed that as in the case of isatin series, the lack of carbonyl group results in loss of hCB₂ functional activity for benzofuran-scaffold-based agonist compounds. The R2 moiety (Table 1) was orientated such that the carbonyl group could possibly make hydrogen bond interactions with S3.31 or Y5.39 as suggested in earlier studies described above. These two conformations were seeded into the pocket and used as the starting structures for the ligand-steered modeling of the binding site. An initial ensemble of 200 structures for each conformation was generated by randomizing the position and orientation of the ligand, followed by a flexible-ligand:flexible-receptor docking procedure to select the most promising complexes (see Methods for a description of this methodology). From these, two representative structures were chosen, the binding sites were visually inspected, and the final complex was retained in which the R1 group was

oriented toward the lipophilic pocket as described earlier and the carbonyl was positioned close enough to any residue side chain to form a hydrogen bond. As described earlier, since we hypothesized that the absence of the carbonyl group resulted in lack of affinity for benzofuran compounds, we assumed that absence of hydrogen-bond interaction with the carbonyl possibly was related to a wrong pose.

Correlation between ligand binding to the CB₂ structural model and SAR data

Given the limited and inconclusive experimental evidence available to validate our model, we evaluated the accuracy of the model by assessing its ability to explain the SAR data of our compounds. In our representative model with compound **33** (Figure 4), the carbonyl group is located at 1.8 Å from the side chain of S3.31, suggesting a possible ligand-receptor interaction via hydrogen bond, as described in earlier studies⁶². Mutagenesis of S3.31 with glycine (S3.31G) and/or F5.46 with valine (F5.46 V) in CB₂ resulted in loss of affinity/activity for several CB₂ agonists, which confirmed the role of these residues in developing CB₂-selective agonists.^[62,95, 96,98] The R1 group (Table 1) is properly located in the aromatic pocket to form van der Waals interactions with residues F5.46 and W6.48. The R2 group (1-piperidyl for compound **33**) is oriented towards F7.35. These observations suggest the overall binding mode and possible ligand receptor interactions of the benzofuran series of agonist compounds. It is important to note the difference in functional activity with different R1 moieties facing the aromatic domain. Introduction of chlorine (compound **30**) at the phenyl ring facing the aromatic pocket results in increased hCB₂ functional activity compared with compound **33**, while introduction of polar moieties such as methoxyphenyl (compound **31**) or 4-pyridine (compound **32**) in the aromatic pocket causes unfavorable interactions with F5.46 and W6.48, resulting in loss of CB₂ functional activity. Decreasing negative electrostatic potential of phenyl ring by introduction of a chlorine (compound **30**) might result in an increase of the pi-stacking interaction with the electron-rich W6.48. Alkenyl moiety (compound **19**) seems to be well tolerated in the aromatic pocket. Introduction of bulky moiety such as 1-naphthyl at the R1 position with 1-piperidyl at R2 (compound **28**) causes steric clashes of the naphthyl group with side chains in TM3, which results in complete loss of hCB₂ functional activity. For compound **29**: the 2-naphthyl group is oriented deeper into the aromatic pocket, which abolishes the pi-stacking interaction with W6.48 and possibly the hydrogen bond interaction with S3.31, which explains its loss of activity.

Combination of a cyclohexyl ring at R2 with a 1-naphthyl ring at R1 causes steric clashes with residues in transmembrane 3 and F7.35 and disruption of the hydrogen bond with S3.31, explaining the complete loss of CB₂ functional activity for compound **27**. As the aromatic pocket formed by residues F5.46 and W6.48 was well suited to tolerate either an alkene or a phenyl ring, we decided to explore the receptor-ligand interactions for R2, keeping either an alkene or a phenyl group for R1. Replacing the piperidine ring of compound **19** by a cyclohexylamine ring (**20**) results in direct steric clashes with F7.35 and decrease of CB₂ functional activity. Moving the carboxamide moiety from position 6 to position 5 (compounds **13–15**) results in loss of hydrogen-bond interaction with S3.31, explaining dramatic loss of CB₂ functional activity of these compounds. The same disruption of the hydrogen bond with S3.31 by steric clashes between F7.35 and the bulky iodoaniline ring might explain the loss of activity for compound **16**. However, some activity is regained when the iodoaniline ring is replaced by a cyclohexyl group (compound **17**). On the other hand, neopentylamine moiety (compound **21**) or *N*-tert-butylmethylamine moiety (compound **23**) exhibited the same range of CB₂ potency as the piperidine analog **18**. It should be noted that compound **21** showed an efficacy of 48 %. As the vicinity of the R2 moiety is lipophilic, the lower lipophilicity of the neopentylamine nitrogen (compound **21**) compared to the trisubstituted piperidine nitrogen (compound **18**) or *N*-tert-butylmethylamine

(compound **23**) might explain the decrease of CB₂ efficacy. Introduction of a morpholine ring in compound **22** disrupts the aromatic interactions with F7.35 and possibly hydrogen bond with S3.31, explaining the loss of CB₂ functional activity. However, replacing the morpholine ring by a methyltetrahydropyran (compound **24**) restores some CB₂ functional activity. The additional flexibility of the methyltetrahydropyran ring compared to the morpholine group might result in exposing compound **24** to the solvent. For compound **34**, the *R* en-antiomer of compound **33**, accommodation of the phenyl group in the aromatic binding pocket results in a flipped benzofuran core, which may explain the decreased activity.

Some compounds were selected for binding studies at hCB₁ and hCB₂ (Table 2). Compounds **20** allow us to rule out any potential CB₂ antagonist activity. Binding results were in agreement with the corresponding hCB₂ functional activities. Both compound **20** and compound **30** exhibited CB₂ affinity in agreement with the corresponding CB₂ functional activities. Compound **18** would be expected to show the same range of affinity for CB₂ as compounds **19** and **30** according to the hCB₂ functional activities. However, the CB₂ affinity of compound **18** was four times lower, which might be explained by a different positioning of the radiolabeled ligand in the receptor compared with compound **18**.

Effects of compounds **19** and **1** on tactile allodynia in a paclitaxel-induced neuropathic pain model

Tactile allodynia developed in 100 % of rats 10 days after the start of paclitaxel administration. In paclitaxel-treated rats, intraperitoneal administration of compound **19** suppressed mechanical allodynia (Figure 5) in a dose-dependent manner. The %MPE (maximum peak effect) for reversing mechanical allodynia for the 15 mg kg⁻¹ compound **19** dose was significantly different (*P* < 0.05) from that of the vehicle.

The effects of 1 mg kg⁻¹, 3 mg kg⁻¹, and 5 mg kg⁻¹ of compound **1**, a CB₂ ligand,^[103] were not significantly different from the effects induced by the vehicle (Figure 5). The antinociceptive effects of compound **1** have been shown to involve the μ-opioid receptor system and β-endorphin and to be blocked by administration of the opioid receptor antagonist naloxone or antiserum to β-endorphin.^[7, 104]

ADMET

Because the complete pharmacological profile was completed for compound **18**,^[7] we performed ADME-Tox assessment for compound **18**. No main issues appeared in the preliminary compound-**18** profile (Table 3). Aqueous solubility and plasma protein binding are in the range of those of many marketed drugs. The partition coefficient (Log D, n-octanol/PBS, pH 7.4) was not determined because compound **18** was below the limit of quantitation in the aqueous phase. Intestinal permeability is compatible with oral administration with no efflux. The Ames test was performed to determine whether compound **18** was mutagenic. No genetic toxicity up to 10 μm was detected (Table 3).^[86] Compound **18** did not show any cardiac toxicity.

Conclusions

In summary, we have discovered a novel series of CB₂ agonists that are potent and selective. A multidisciplinary approach was carried out with the aim of improving understanding of the interaction between our new series of compounds and the cannabinoid receptor CB₂. Organic synthesis, enantiomer separation, configurational assignment, and in vitro biological testing were carried out and validated our CB₂ homology model. Compound **33** and compound **34**, the two enantiomers of compound **18**, were tested at CB₂ and CB₁. The *S*

enantiomer, compound **33**, is responsible for compound **18** CB₂ activity, and the *R* enantiomer, compound **34**, exhibited weak CB₂ functional activity. The discrimination between the two enantiomers for CB₂ functional activity was predicted by our homology model. Compound **18** exhibited the best selectivity at CB₂ compared to CB₁. Compound **19** and compound **30** were the most potent at CB₂. Compound **19** was active in a model of neuropathic pain in the same range as compound **18**. Preliminary ADME-Tox studies for compound **18** were performed and did not show any issues. Thus, we have identified a novel series of compounds from which it should be possible to develop new drugs for the treatment of neuropathic pain. Pharmacokinetic and metabolism studies are ongoing for compound **18**.

Experimental Section

All chemicals were purchased from Sigma–Aldrich or Acros. Thin-layer chromatographic analyses were performed on Sigma–Aldrich 60 F₂₅₄ TLC plates. Column chromatography was performed with silica gel (230–400 mesh). ¹H and ¹³C NMR spectra were recorded on Bruker 300 and 500 MHz DPX NMR spectrometers, respectively. Chemical shifts (δ , in ppm) are reported relative to either residual dimethyl sulfoxide (DMSO; 3.35 ppm) or CHCl₃ (7.24 ppm) as internal standards. Signals are abbreviated as follows: br=broad, s=singlet, d=doublet, t=triplet, q=quadruplet, m=multiplet. Coupling constants (*J*) are expressed in Hertz. When needed, the reactions were performed under a positive pressure of dry N₂ gas.

3-Iodo-4-(2-methylallyloxy)benzoic acid methyl ester (**10 a**)

Finely powdered K₂CO₃ (1.49 g, 10.78 mmol) was added to a solution of methyl 4-hydroxy-3-iodobenzoate (1.5 g, 5.4 mmol) in anhydrous methyl ethyl ketone (60 mL) followed by 3-bromo-2-methylpropene (0.81 mL, 1.1 g, 8.15 mmol). The reaction mixture was heated at 70°C for 4 h. The mixture was diluted with EtOAc and filtered. The filtrate was washed with H₂O and dried over MgSO₄. Evaporation of the solvent and of the remaining bromopropene under vacuum afforded 1.77 g (98 %) of pure **10a** as a yellow oil. ¹H NMR (300 MHz, CDCl₃): δ = 8.46 (d, *J* = 1.8 Hz, 1 H), 7.98 (dd, *J* = 8.7 Hz, *J* = 1.8 Hz, 1 H), 6.80 (d, *J* = 8.7 Hz, 1 H), 5.19 (d, *J* = 1.2 Hz, 1 H), 5.04 (d, *J* = 1.2 Hz, 1 H), 4.54 (s, 2H), 3.09 (s, 3H), 1.88 (d, *J* = 1.2 Hz, 3H); ¹³C NMR (500 MHz, CDCl₃): δ = 165.49 (C=O), 160.64 (C), 140.99 (CH), 139.52 (C), 131.44 (CH), 113.39 (CH₂), 111.09 (CH), 90.50 (C), 72.71 (CH₂), 52.10 (CH₃), 19.41 (CH₃).

4-Iodo-3-(2-methylallyloxy)benzoic acid methyl ester (**10 b**)

Methyl 3-hydroxy-4-iodobenzoate (1.5 g, 5.4 mmol) was submitted to the same procedure described above for the preparation of **10 a**. Evaporation of the solvent and of the remaining bromopropene under vacuum afforded 1.4 g (78 %) of pure **10 b** as a yellow oil. ¹H NMR (500 MHz, CDCl₃): δ = 7.86 (d, *J* = 8.1 Hz, 1 H), 7.42 (d, *J* = 1.7 Hz, 1H), 7.36 (dd, *J* = 8.1 Hz, 1.8 Hz, 1 H), 5.23 (s, 1H), 5.04 (s, 1 H), 4.54 (s, 2 H), 3.91 (s, 3 H), 1.88 (s, 3H); ¹³C NMR (500 MHz, CDCl₃): δ = 166.58 (C=O), 157.24 (C), 139.78 (C), 139.52 (CH), 131.49 (C), 123.36 (CH), 113.25 (CH₂), 112.43 (CH), 93.22 (C), 72.68 (CH₂), 52.31 (CH₃), 19.50 (CH₃).

3-Benzyl-3-methyl-2,3-dihydrobenzofuran-5-carboxylic acid methyl ester (**11 a**)

K₂CO₃ (379 mg, 2.74 mmol), tetra-*n*-butylammonium chloride (380 mg, 1.37 mmol), and PhB(OH)₂ (200 mg, 1.64 mmol) were added to a solution of **10a** (455 mg, 1.37 mmol) in DMF (15 mL). The resulting mixture was heated at 115°C, and [Pd(OAc)₂] (25.6 mg, 0.136 mmol) dissolved in DMF (5 mL) was added. The resulting mixture was stirred for 3 h at 115 °C, cooled to room temperature, filtered over silica, washed with H₂O, dried over MgSO₄,

and concentrated under vacuum. Column chromatography (silica gel, heptane/CH₂Cl₂ 4:6) afforded 202 mg (52%) of the title compound as a light brown oil. ¹H NMR (300 MHz, CDCl₃): δ = 7.89 (dd, *J* = 8.4, 1.8, 1H), 7.72 (d, *J* = 1.8 Hz, 1H), 7.23 (m, 3H), 6.98 (m, 2H), 6.74 (d, *J* = 8.4 Hz, 1H), 4.60 (d, *J* = 8.9 Hz, 1H), 4.13 (d, *J* = 8.9 Hz, 1H), 3.89 (s, 3H), 2.93 (d, *J* = 13.4 Hz, 1H), 2.87 (d, *J* = 13.4 Hz, 1H), 1.40 (s, 3H); ¹³C NMR (75 MHz, CDCl₃): δ = 167.00 (C=O), 163.75 (C), 137.06 (C), 135.39 (C), 131.25 (CH), 130.22 (CH), 128.08 (CH), 126.67 (CH), 125.23 (CH), 122.70 (C), 109.45 (CH), 82.56 (CH₂), 51.83 (CH₃), 46.66 (CH₂), 45.93 (C), 25.04 (CH₃).

3-Benzyl-3-methyl-2,3-dihydrobenzofuran-6-carboxylic acid methyl ester (11 b)

Compound **10b** (455 mg, 1.37 mmol) was submitted to the same procedure described above for the preparation of **11 a**. Column chromatography (silica gel, heptane/CH₂Cl₂ 4:6) afforded 368 mg (95 %) of the title compound as a light brown oil that crystallized; mp: 52°C; ¹H NMR (500 MHz, CDCl₃): δ = 7.59 (dd, *J* = 7.7 Hz, 1.2 Hz, 1H), 7.39 (d, *J* = 1.0 Hz, 1H), 7.22 (m, 3H), 6.96 (m, 3H), 4.54 (d, *J* = 8.7 Hz, 1H), 4.11 (d, *J* = 8.7 Hz, 1H), 3.89 (s, 3H), 2.88 (q, *J* = 13.3, 2H), 1.37 (s, 3H); ¹³C NMR (500 MHz, CDCl₃): δ = 167.06 (C=O), 159.73 (C), 140.30 (C), 137.01 (C), 130.53 (C), 130.34 (CH), 128.05 (CH), 126.68 (CH), 123.19 (CH), 122.41 (CH), 110.64 (CH), 82.33 (CH₂), 52.13 (CH₃), 46.43 (CH₂), 46.39 (C), 24.46 (CH₃).

3-((E)-Hex-2-enyl)-3-methyl-2,3-dihydrobenzofuran-6-carboxylic acid methyl ester (11 c)

Compound **10 b** (65 mg, 0.2 mmol) was submitted to the same procedure described above for the preparation of **11 a** using 1-penten-1-ylboronic acid (26 mg, 0.23 mmol). Column chromatography (silica gel, heptane/CH₂Cl₂ 6:4) afforded 290 mg (48%) of the title compound as a light yellow oil. ¹H NMR (500 MHz, CDCl₃): δ = 7.60 (dd, *J* = 7.7 Hz, 1.4 Hz, 1H), 7.40 (d, *J* = 1.1 Hz, 1H), 7.11 (d, *J* = 7.7 Hz, 1H), 5.41–5.47 (m, 1H), 5.31–5.21 (m, 1H), 4.43 (d, *J* = 8.6 Hz, 1H), 4.16 (d, *J* = 8.6 Hz, 1H), 3.89 (s, 3H), 2.35–2.23 (m, 2H), 1.94 (q, *J* = 7.1, 2H), 1.33 (m, 6H), 0.85 (t, *J* = 7.4, 3H); ¹³C NMR (500 MHz, CDCl₃): δ = 167.04 (C=O), 159.73 (C), 140.74 (C), 135.03 (CH), 130.35 (C), 124.68 (CH), 122.66 (CH), 122.49 (CH), 110.46 (CH), 82.28 (CH₂), 52.08 (CH₃), 45.50 (C), 43.65 (CH₂), 34.66 (CH₂), 25.01 (CH₃), 22.54 (CH₂), 13.57 (CH₃).

3-Benzyl-3-methyl-2,3-dihydrobenzofuran-5-carboxylic acid (12 a)

A mixture of compound **10 a** (125 mg, 0.44 mmol), NaOH (120 mg, 3 mmol), EtOH (6 mL), and H₂O (1 mL) in THF (6 mL) was stirred for 12 h at room temperature. The reaction medium was acidified by adding a solution of 1.2M HCl and was extracted with EtOAc. The organic phase was washed with H₂O, dried (Na₂SO₄), and concentrated in a rotary evaporator. The product was obtained as a light brown oil (116 mg, 97 %); ¹H NMR (300 MHz, CDCl₃): δ = 11.43 (s, 1H), 7.89 (dd, *J* = 8.4 Hz, 1.8 Hz, 1H), 7.69 (d, *J* = 1.6 Hz, 1H), 7.11–7.14 (m, 3H), 6.87 (dd, *J* = 6.4 Hz, 2.9 Hz, 2H), 6.67 (d, *J* = 8.4 Hz, 1H), 4.51 (d, *J* = 8.9 Hz, 1H), 4.05 (d, *J* = 8.9 Hz, 1H), 2.83 (d, *J* = 13.4 Hz, 1H), 2.77 (d, *J* = 13.3 Hz, 1H), 1.30 (s, 3H); ¹³C NMR (75 MHz, CDCl₃): δ = 172.34 (C=O), 164.61 (C), 136.99 (C), 134.45 (C), 132.25 (CH), 130.28 (CH), 128.15 (CH), 126.77 (CH), 125.99 (CH), 121.85 (C), 109.69 (CH), 82.81 (CH₂), 46.69 (CH₂), 45.91 (C), 25.04 (CH₃).

3-Benzyl-3-methyl-2,3-dihydrobenzofuran-6-carboxylic acid (12 b)

Compound **11 b** (300 mg, 1.06 mmol) was submitted to the same procedure described above for the preparation of **12 a**. The product was obtained as a white solid (300 mg, 100 %); mp: 165 °C; ¹H NMR (500 MHz, CDCl₃): δ = 7.67 (dd, *J* = 7.7 Hz, 1.3 Hz, 1H), 7.46 (d, *J* = 1.0 Hz, 1H), 7.22–7.25 (m, 3H), 7.02–6.94 (m, 3H), 4.57 (d, *J* = 8.7 Hz, 1H), 4.14 (d, *J* = 8.7 Hz, 1H), 2.91 (q, *J* = 13.4 Hz, 2H), 2.87 (q, *J* = 13.4 Hz, 2H), 1.39 (s, 3H); ¹³C NMR (500

MHz, CDCl₃): δ = 171.61 (C=O), 159.79 (C), 141.33 (C), 136.92 (C), 130.34 (CH), 129.61 (C), 128.08 (CH), 126.73 (CH), 123.31 (CH), 123.11 (CH), 111.14 (CH), 82.37 (CH₂), 46.45 (C), 46.41 (CH₂), 24.43 (CH₃).

3-((*E*-Hex-2-enyl)-3-methyl-2,3-dihydrobenzofuran-6-carboxylic acid (12 c)

Compound **11 c** (200 mg, 0.73 mmol) was submitted to the same procedure described above for the preparation of **12 a**. The product was obtained as a colorless oil (155 mg, 82%) that crystallized. mp: 172–173°C; ¹H NMR (500 MHz, CDCl₃): δ =7.70 (dd, *J*=7.7 Hz, 1.2 Hz, 1 H), 7.49 (d, *J*=0.9 Hz, 1 H), 7.17 (d, *J*=7.7 Hz, 1H), 5.48 (dt, *J*=13.9 Hz, 6.8 Hz, 1 H), 5.30 (dt, *J*=14.9 Hz, 7.3 Hz, 1 H), 4.48 (d, *J*=8.6 Hz, 1 H), 4.20 (d, *J*=8.6 Hz, 1 H), 2.39–2.27 (m, 2 H), 1.98 (dd, *J*=14.1, 7.1 Hz, 2H), 1.42–1.31 (m, 6 H), 0.88 (t, *J*=7.4 Hz, 3H); ¹³C NMR (500 MHz, CDCl₃): δ =170.99 (C=O), 159.79 (C), 141.77 (C), 135.15 (CH), 129.31 (C), 124.58 (CH), 123.21 (CH), 122.81 (CH), 110.96 (CH), 100.00 (C), 82.32 (CH₂), 45.57 (C), 43.63 (CH₂), 34.67 (CH₂), 25.00 (CH₃), 22.54 (CH₂), 13.58 (CH₃).

3-Benzyl-3-methyl-2,3-dihydrobenzofuran-5-carboxylic acid-*o*-iodoanilide (13)

O-(7-Azabenzotriazol-1-yl)-*N,N,N'*-tetramethyluronium hexafluorophosphate (HATU; 94 mg, 0.25 mmol) and a solution of *N,N*-diisopropylethylamine (DiPEA; 44 mg, 59 μ L, 0.34 mmol) in DMF (1 mL) were added to a stirred suspension of compound **12a** (60 mg, 0.225 mmol) and 2-iodoaniline (54 mg, 0.25 mmol) in CH₂Cl₂ (2 mL) and DMF (1 mL). The reaction mixture was stirred at room temperature for 18 h. The reaction medium was acidified by adding a solution of 1.2 M HCl and extracted with EtOAc. The organic phase was washed with H₂O, dried (MgSO₄), and concentrated to give the amide, which was purified by flash chromatography (EtOAc/heptane 4:6) to afford 10 mg (10%) of a light brown oil. ¹H NMR (300 MHz, CDCl₃): δ = 8.75 (dd, *J* = 4.4 Hz, 1.3 Hz, 1 H), 8.47 (dd, *J* = 8.4 Hz, 1.4 Hz, 1H), 8.17 (dd, *J* = 8.6 Hz, 2.0 Hz, 1H), 7.90 (d, *J* = 1.9 Hz, 1H), 7.47 (dd, *J* = 8.4 Hz, 4.5 Hz, 1H), 7.28–7.22 (m, 4H), 7.01 (dd, *J* = 7.4 Hz, 1.7 Hz, 2 H), 6.89 (d, *J* = 8.5 Hz, 1 H), 4.70 (d, *J* = 9.1 Hz, 1 H), 4.24 (d, *J* = 9.1 Hz, 1 H), 2.98 (d, *J* = 13.3 Hz, 1H), 2.91 (d, *J* = 13.3 Hz, 2H), 1.45 (s, 3H).

3-Benzyl-3-methyl-2,3-dihydrobenzofuran-5-carboxylic acid cyclohexylamide (14)

Compound **12 a** (60 mg, 0.225 mmol) was submitted to the same procedure described above for the preparation of **13** using cyclohexylamine (25 mg, 29 μ L, 0.25 mmol). The organic phase was washed with H₂O, dried (MgSO₄), and concentrated to give the amide as a white solid. The solid was washed with a mixture of heptane and CH₂Cl₂/heptanes (9:1) to afford 38 mg (48 %) of a white solid. ¹H NMR (300 MHz, CDCl₃): δ = 7.56 (dd, *J* = 8.3, 1.9, 1H), 7.24 (dd, *J* = 5.0 Hz, 1.9 Hz, 4H), 6.98 (dd, *J* = 6.5 Hz, 2.8 Hz, 2 H), 6.75 (d, *J* = 8.3 Hz, 1 H), 5.72 (d, *J* = 7.4 Hz, 1 H), 4.57 (d, *J* = 8.9 Hz, 1H), 4.14 (d, *J* = 8.8 Hz, 1 H), 4.03–3.86 (m, 1 H), 2.93 (d, *J* = 13.3 Hz, 1H), 2.86 (d, *J* = 13.2 Hz, 1 H), 2.00–2.04 (m, 1 H), 1.83–1.53 (m, 4H), 1.52–1.32 (m, 5 H), 1.32–1.11 (m, 3H); ¹³C NMR (500 MHz, CDCl₃): δ = 166.39 (C=O), 162.24 (C), 137.21 (C), 135.12 (C), 130.44 (CH), 127.96 (CH), 127.77 (CH), 127.41 (C), 126.68 (CH), 122.79 (CH), 109.34 (CH), 82.83 (CH₂), 48.59 (CH), 46.64 (C), 46.06 (CH₂), 33.34 (CH₂), 25.64 (CH₂), 24.95 (CH₂), 24.68 (CH₃); HRMS (ES⁺) calcd for C₂₃H₂₇NO₂ [*M*+H]⁺ *m/z*: 350.2120, found: 350.2095.

3-Benzyl-3-methyl-2,3-dihydrobenzofuran-5-carboxylic acid piperidine amide (15)

Compound **12 a** (60 mg, 0.225 mmol) was submitted to the same procedure described above for the preparation of **13** using piperidine (21 mg, 25 μ L, 0.25 mmol). The organic phase was washed with H₂O, dried (MgSO₄), and concentrated to give the amide, which was purified by flash chromatography (EtOAc/heptane 3:7) to afford 54 mg (71.5%) of the desired amide as a colorless oil. ¹H NMR (300 MHz, CDCl₃): δ = 7.25–7.16 (m, 4 H), 7.03

(d, $J=1.7$, 1H), 6.99 (dd, $J=8.2$ Hz, 1.7 Hz, 2 H), 6.73 (d, $J=8.2$ Hz, 1 H), 4.53 (t, $J=8.4$ Hz, 1 H), 4.10 (d, $J=8.4$ Hz, 1 H), 3.53 (br s, 4H), 2.92 (d, $J=13.3$ Hz, 1 H), 2.86 (d, $J=13.3$ Hz, 1 H), 1.75–1.48 (m, 6 H), 1.37 (s, 3 H); ^{13}C NMR (500 MHz, CDCl_3): δ = 170.77 (C=O), 160.80 (C), 137.37 (C), 135.14 (C), 130.44 (CH), 128.68 (C), 128.16 (CH), 128.02 (CH), 126.72 (CH), 123.05 (CH), 109.42 (CH), 82.58 (CH_2), 46.68 (CH_2), 46.32 (C), 29.84 (CH_2), 24.81 (CH_2), 24.72 (CH_3); HRMS (ES +) calcd for $\text{C}_{22}\text{H}_{25}\text{NO}_2$ [$M+\text{H}$] $^+$ m/z : 336.1964, found: 336.1932.

3-Benzyl-3-methyl-2,3-dihydrobenzofuran-6-carboxylic acid (2-iodophenyl)amide (16)

Compound **12b** (80 mg, 0.3 mmol) was submitted to the same procedure described above for the preparation of **13** using 2-iodoaniline (72 mg, 0.33 mmol). The crude amide was purified by flash chromatography (EtOAc/heptane 4:6) to afford 22 mg of the desired amide as a pale yellow solid (16%). ^1H NMR (300 MHz, CDCl_3): δ = 8.74 (dd, $J=4.5$ Hz, 1.4 Hz, 1 H), 8.46 (dd, $J=8.4$ Hz, 1.4 Hz, 1H), 7.85 (dd, $J=7.8$ Hz, 1.5 Hz, 1H), 7.61 (d, $J=1.3$ Hz, 1H), 7.46 (dd, $J=8.4$ Hz, 4.5 Hz, 1H), 7.29–7.26 (m, 2 H), 7.07 (d, $J=7.8$ Hz, 1H), 6.99 (dd, $J=6.4$ Hz, 3.0 Hz, 2H), 4.62 (d, $J=8.9$ Hz, 1H), 4.21 (d, $J=8.9$ Hz, 1 H), 2.98 (d, $J=13.3$ Hz, 1 H), 2.92 (d, $J=13.4$ Hz, 1 H), 1.44 (s, 3H); ^{13}C NMR (500 MHz, CDCl_3): δ = 165.41 (C=O), 160.38 (C), 139.73 (C), 138.99 (C), 138.52 (CH), 137.12 (C), 135.27 (C), 130.54 (CH), 129.57 (CH), 128.27 (CH), 126.91 (CH), 126.17 (CH), 124.01 (CH), 121.96 (CH), 119.93, 108.64 (CH), 90.39 (C-I), 82.72 (CH_2), 46.63(C), 46.56 (CH_2), 24.74 (CH_3); HRMS (ES +) calcd for $\text{C}_{23}\text{H}_{20}\text{INO}_2$ [$M+\text{H}$] $^+$ m/z : 470.0617, found: 470.0638.

3-Benzyl-3-methyl-2,3-dihydrobenzofuran-6-carboxylic acid cyclohexylamide (17)

Compound **12b** (80 mg, 0.3 mmol) was submitted to the same procedure described above for the preparation of **13** using cyclohexylamine (33 mg, 38 μL , 0.33 mmol). Crude amide was purified by flash chromatography (EtOAc/heptane 2:8) to afford 70 mg (67 %) of a white solid; mp: 119–121 $^\circ\text{C}$; ^1H NMR (300 MHz, CDCl_3): δ = 7.28–7.20 (m, 6 H), 7.11 (d, $J=1.4$ Hz, 1H), 6.98 (dd, $J=6.4$ Hz, 3.1 Hz, 2 H), 6.92 (d, $J=7.7$ Hz, 1H), 5.87 (d, $J=6.8$ Hz, 1 H), 4.54 (d, $J=8.8$ Hz, 1 H), 4.11 (d, $J=8.8$ Hz, 1H), 4.03–3.88 (m, 1 H), 2.91 (d, $J=13.3$ Hz, 1H), 2.86 (d, $J=13.3$ Hz, 1 H), 2.02 (m, 2 H), 1.82–1.60 (m, 3 H), 1.52–1.32 (m, 5H), 1.31–1.13 (m, 3 H); ^{13}C NMR (500 MHz, CDCl_3): δ = 166.48 (C=O), 159.88 (C), 138.29 (C), 137.08 (C), 135.76 (C), 130.36 (CH), 128.03 (CH), 126.62 (CH), 123.39 (CH), 119.31 (CH), 108.17 (CH), 82.46 (CH_2), 48.64 (CH), 46.43 (CH_2), 46.26 (C), 33.23 (CH_2), 25.59 (CH_2), 24.90 (CH_2), 24.59 (CH_3); HRMS (ES+) calcd for $\text{C}_{23}\text{H}_{27}\text{NO}_2$ [$M+\text{H}$] $^+$ m/z : 350.2120, found: 350.2090.

3-Benzyl-3-methyl-2,3-dihydrobenzofuran-6-carboxylic acid piperidine amide (18)

Compound **12b** (80 mg, 0.3 mmol) was submitted to the same procedure described above for the preparation of **13** using piperidine (28 mg, 33 μL , 0.33 mmol). Crude amide was purified by flash chromatography (EtOAc/heptane 4:6) to afford 50 mg (50%) of a white solid; mp: 108 $^\circ\text{C}$; ^1H NMR (500 MHz, CDCl_3): δ = 7.25–7.20 (m, 3H), 7.00 (dd, $J=7.0$ Hz, 1.2 Hz, 2H), 6.94 (d, $J=7.5$ Hz, 1 H), 6.89 (dd, $J=7.5$ Hz, 1.2 Hz, 1 H), 6.75 (d, $J=0.7$ Hz, 1H), 4.53 (d, $J=8.7$ Hz, 1H), 4.09 (d, $J=8.7$ Hz, 1H), 3.41 (br s, 2 H), 3.69 (br s, 2 H), 2.90 (d, $J=13.3$ Hz, 1H), 2.86 (d, $J=13.3$ Hz, 1H), 1.71–1.46 (m, 6H), 1.36 (s, 3H); ^{13}C NMR (500 MHz, CDCl_3): δ = 170.18 (C=O), 159.47 (C), 137.26 (C), 136.76 (C), 136.20 (C), 130.36 (CH), 127.99 (CH), 126.58 (CH), 123.42 (CH), 119.08 (CH), 108.20 (CH), 82.28 (CH_2), 46.56 (CH_2), 46.22 (C), 24.64 (CH_2), 24.56 (CH_3); HRMS (ES +) calcd for $\text{C}_{22}\text{H}_{25}\text{NO}_2$ [$M+\text{H}$] $^+$ m/z : 336.1964, found: 336.1964.

3-((E)-Hex-2-enyl)-3-methyl-2,3-dihydrobenzofuran-6-yl]piperidin-1-ylmethanone (19)

Compound **12c** (70 mg, 0.27 mmol) was submitted to the same procedure described above for the preparation of **13** using piperidine (25 mg, 0.29 mmol). Crude amide was purified by flash chromatography (EtOAc/heptane 3:7) to afford 69 mg (78%) of a colorless oil. ¹H NMR (300 MHz, CDCl₃): δ = 7.07 (d, *J* = 7.5 Hz, 1 H), 6.89 (dd, *J* = 7.5 Hz, 1.4 Hz, 1 H), 6.77 (d, *J* = 1.0 Hz, 1H), 5.50–5.41 (dt, *J* = 13.8 Hz, 6.8 Hz, 1 H), 5.35–5.24 (m, 1 H), 4.41 (d, *J* = 8.6 Hz, 1 H), 4.13 (d, *J* = 8.6 Hz, 1H), 3.68 (s, 2 H), 3.35 (s, 2 H), 2.28 (d, *J* = 7.1 Hz, 2 H), 1.96 (dd, *J* = 14.0 Hz, 7.1 Hz, 2 H), 1.76–1.58 (m, 6 H), 1.42–1.23 (m, 4H), 0.86 (t, *J* = 7.3 Hz, 3 H); ¹³C NMR (500 MHz, CDCl₃): δ = 170.27 (C=O), 159.48 (C), 136.62 (C), 136.52 (C), 134.80 (CH), 124.96 (CH), 122.99 (CH), 119.14 (CH), 108.06 (CH), 82.28 (CH₂), 45.31 (C), 43.70 (CH₂), 34.67 (CH₂), 25.16 (CH₃), 24.64 (CH₂), 22.58 (CH₂), 13.61 (CH₃); HRMS (ES +) calcd for C₂₁H₂₉NO₂ [M+H]⁺ *m/z*: 328.2277, found: 328.2247.

3-((E)-Hex-2-enyl)-3-methyl-2,3-dihydrobenzofuran-6-carboxylic acid cyclohexylamide (20)

Compound **12c** (70 mg, 0.27 mmol) was submitted to the same procedure described above for the preparation of **13** using cyclohexylamine (30 mg, 0.3 mmol). Crude amide was purified by flash chromatography (EtOAc/heptane 2:8) to afford 83 mg (90%) of a colorless oil. ¹H NMR (300 MHz, CDCl₃): δ = 7.27 (dd, *J* = 7.7 Hz, 1.3 Hz, 1 H), 7.12 (d, *J* = 1.3 Hz, 1H), 7.09 (d, *J* = 7.7 Hz, 1H), 5.86 (br d, *J* = 8.5 Hz, 1 H), 5.51–5.39 (m, 1 H), 5.33–5.20 (m, 1 H), 4.42 (d, *J* = 8.7 Hz, 1H), 4.15 (d, *J* = 8.7 Hz, 1H), 4.04–3.87 (m, 1 H), 2.34–2.23 (m, 2H), 2.10–1.89 (m, 4H), 1.81–1.69 (m, 4 H), 1.52–1.13 (m, 9H), 0.85 (t, *J* = 7.3 Hz, 3H); ¹³C NMR (500 MHz, CDCl₃): δ = 165.06 (C=O), 158.36 (C), 137.23 (C), 134.08 (C), 133.41 (CH), 123.25 (CH), 121.35 (CH), 117.83 (CH), 106.49 (CH), 80.83 (CH₂), 47.06 (CH₃), 43.83 (CH₂), 42.13 (C), 33.14 (CH₂), 31.70 (CH₂), 28.17 (CH₂), 24.05 (CH₂), 23.60 (CH₃), 23.35 (CH₂), 21.02 (CH₂), 12.07 (CH₃); HRMS (ES +) calcd for C₂₂H₃₁NO₂ [M+H]⁺ *m/z*: 342.2433, found: 342.2463.

3-Benzyl-3-methyl-2,3-dihydrobenzofuran-5-carboxylic acid (2,2-dimethylpropyl)amide (21)

Compound **12b** (60 mg, 0.225 mmol) was submitted to the same procedure described above for the preparation of **13** using neopentylamine (29 mg, 0.33 mmol). Crude amide was purified by flash chromatography (EtOAc/heptane 2:8) to afford 53 mg (60 %) of a colorless oil. ¹H NMR (500 MHz, CDCl₃): δ = 7.29 (dd, *J* = 7.7 Hz, 1.3 Hz, 1H), 7.25–7.22 (m, 3 H), 7.13 (d, *J* = 1.1 Hz, 1 H), 6.99 (dd, *J* = 7.0 Hz, 2.0 Hz, 2H), 6.94 (d, *J* = 7.7 Hz, 1H), 6.08 (s, 1H), 4.55 (d, *J* = 8.7 Hz, 1H), 4.12 (d, *J* = 8.7 Hz, 1H), 3.26 (d, *J* = 6.3 Hz, 2 H), 2.91 (d, *J* = 13.4 Hz, 1 H), 2.87 (d, *J* = 13.3 Hz, 1H), 1.37 (s, 3H), 0.98 (s, 9 H); ¹³C NMR (500 MHz, CDCl₃): δ = 167.56 (C=O), 159.91 (C), 138.43 (C), 137.06 (C), 135.70 (C), 130.37 (CH), 128.04 (CH), 126.65 (CH), 123.50 (CH), 119.36 (CH), 108.11 (CH), 82.48 (CH₂), 51.00 (CH₂), 46.42 (CH₂), 46.28 (C), 32.15 (C), 27.30 (CH₃), 24.58 (CH₃); HRMS (ES +) calcd for C₂₂H₂₇NO₂ [M+H]⁺ *m/z*: 338.2120, found: 338.2148.

(3-Benzyl-3-methyl-2,3-dihydrobenzofuran-6-yl)morpholinomethanone (22)

Compound **12b** (70 mg, 0.26 mmol) was submitted to the same procedure described above for the preparation of **13** using morpholine (48 mg, 0.56 mmol). Crude amide was purified by flash chromatography (EtOAc/heptane 4:6) to afford 56 mg (64 %) of a colorless oil. ¹H NMR (300 MHz, CDCl₃): δ = 7.22–7.24 (m, 2 H), 7.00–7.02 (m, 2H), 6.96 (d, *J* = 7.5 Hz, 1 H), 6.90 (dd, *J* = 7.6 Hz, 1.3, 1H), 6.76 (d, *J* = 0.9 Hz, 1H), 4.54 (d, *J* = 8.8 Hz, 0 H), 4.10 (d, *J* = 8.8 Hz, 0 H), 3.59 (br m, 4H), 2.91 (d, *J* = 13.4 Hz, 1 H), 2.85 (d, *J* = 13.4 Hz, 1 H), 1.36 (s, 3 H); ¹³C NMR (500 MHz, CDCl₃): δ = 170.34 (C=O), 159.58 (C), 137.13 (C), 136.85 (C), 135.50 (C), 130.34 (CH), 128.01 (CH), 126.63 (CH), 123.61 (CH), 119.38 (CH), 108.44 (CH), 82.35 (CH₂), 66.92 (CH₂), 46.51 (C), 46.24, 24.56 (CH₃); HRMS (ES +) calcd for C₂₁H₂₃NO₃ [M+H]⁺ *m/z*: 338.1756, found: 338.1763.

3-Benzyl-*N*-*tert*-butyl-*N*,3-dimethyl-2,3-dihydrobenzofuran-6-carboxamide (23)

Compound **12 b** (70 mg, 0.26 mmol) was submitted to the same procedure described above for the preparation of **13** using *N*-*tert*-butylmethylamine (29 mg, 0.29 mmol). Crude amide was purified by flash chromatography (EtOAc/heptane 2:8) to afford 69 mg (76%) of an off-white oil; mp: 71 °C; ¹H NMR (300 MHz, CDCl₃): δ = 7.22–7.23 (m, 3 H), 6.99 (dd, *J* = 6.4 Hz, 3.0, 2 H), 6.94 (dd, *J* = 7.6 Hz, 1.3 Hz, 1H), 6.89 (d, *J* = 7.5 Hz, 1H), 6.78 (d, *J* = 1.1 Hz, 1H), 4.52 (d, *J* = 8.8 Hz, 0 H), 4.08 (d, *J* = 8.8 Hz, 0 H), 2.94–2.81 (m, 5H), 1.49 (s, 9H), 1.35 (s, 3 H); ¹³C NMR (500 MHz, CDCl₃): δ = 172.98 (C=O), 159.42 (C), 139.44 (C), 137.26 (C), 136.21 (C), 130.35 (CH), 127.95 (CH), 126.53 (CH), 123.25 (CH), 119.63 (CH), 108.63 (CH), 82.25 (CH₂), 56.42 (C), 46.53 (CH₂), 46.18 (C), 35.34 (CH₃), 27.73 (CH₃), 24.50 (CH₃); HRMS (ES +) calcd for C₂₂H₂₇NO₂ [*M*+H]⁺ *m/z*: 338.2120, found: 338.2147.

3-Benzyl-3-methyl-2,3-dihydrobenzofuran-6-carboxylic acid (tetrahydropyran-4-ylmethyl)amide (24)

Compound **12 b** (70 mg, 0.26 mmol) was submitted to the same procedure described above for the preparation of **13** using 4-(aminomethyl)tetrahydropyran (46 mg, 0.4 mmol). Crude amide was purified by flash chromatography (EtOAc/heptane 5:5) to afford 41 mg (43%) of a colorless oil. ¹H NMR (500 MHz, CDCl₃): δ = 7.28 (dd, *J* = 7.7, 1.4, 1H), 7.23–7.24 (m, 3H), 7.12 (d, *J* = 1.2, 1 H), 6.97 (dd, *J* = 6.9 Hz, 2.4 Hz, 2H), 6.93 (d, *J* = 7.7 Hz, 1H), 6.26 (br s, 1H), 4.54 (d, *J* = 8.7 Hz, 1H), 4.12 (d, *J* = 8.7 Hz, 1 H), 3.98 (dd, *J* = 11.3 Hz, 3.2 Hz, 2H), 3.42–3.31 (m, 4 H), 2.91 (d, *J* = 13.3 Hz, 1 H), 2.86 (d, *J* = 13.3 Hz, 1 H), 1.95–1.82 (m, 1H), 1.66 (d, *J* = 11.6 Hz, 3 H), 1.48–1.27 (m, 5 H); ¹³C NMR (500 MHz, CDCl₃): δ = 167.60 (C=O), 159.95 (C), 138.61 (C), 137.03 (C), 135.20 (C), 130.36 (CH), 128.05 (CH), 126.66 (CH), 123.50 (CH), 119.37 (CH), 108.12 (CH), 82.47 (CH₂), 67.62 (CH₂), 46.43 (CH₂), 46.29 (C), 45.69 (CH₂), 35.39 (CH), 30.70 (CH₂), 24.57 (CH₃); HRMS (ES +) calcd for C₂₃H₂₇NO₃ [*M*+H]⁺ *m/z*: 366.2069, found: 366.2065.

4-Iodo-3-(2-methylallyloxy)benzoic acid (25)

Compound **10 b** (2 g, 6 mmol) was submitted to the same procedure described above for the preparation of **12 a**. The product was obtained as a colorless oil (1.8 g, 94%). ¹H NMR (300 MHz, CDCl₃): δ = 7.91 (d, *J* = 7.9 Hz, 1 H), 7.46 (m, 2 H), 5.23 (s, 1 H), 5.06 (s, 1H), 4.57 (s, 2H), 1.89 (s, 3 H); ¹³C NMR (500 MHz, CDCl₃): δ = 171.43 (C=O), 157.34 (C), 139.75 (CH), 139.69 (C), 130.51 (C), 123.99 (CH), 113.39 (CH₂), 112.73 (CH), 94.62 (C), 72.73 (CH₂), 19.49 (CH₃).

***N*-Cyclohexyl-4-iodo-3-(2-methylallyloxy)benzamide (26 a)**

HATU (449 mg, 1.18 mmol) and then DiPEA (229 mg, 1.77 mmol, 0.31 mL) were added to a stirred suspension of **25** (350 mg 1.1 mmol) and cyclohexylamine (117 mg, 1.18 mmol, 0.134 mL) in CH₂Cl₂ (5 mL) and DMF (5 mL). The reaction mixture was stirred at room temperature for 18 h. The reaction medium was acidified by the addition of a solution of HCl (3.7 %) and extracted with CH₂Cl₂. The organic phase was washed three times with H₂O, dried (MgSO₄), and concentrated to give the crude amide. Column chromatography (silica gel, heptane/EtOAc 7:3) afforded the title compound as a white solid (418 mg, 95 %); mp: 124–126 °C; ¹H NMR (500 MHz, CDCl₃): δ = 7.80 (d, *J* = 8.0 Hz, 1H), 7.29 (d, *J* = 1.7 Hz, 1H), 6.94 (dd, *J* = 8.0 Hz, 1.7 Hz, 1H), 5.93 (d, *J* = 7.4 Hz, 1 H), 5.22 (s, 1 H), 5.04 (s, 1 H), 4.55 (s, 2 H), 4.02–3.90 (m, 1H), 2.03 (dd, *J* = 12.4 Hz, 3.1 Hz, 2 H), 1.87 (s, 3H), 1.80–1.71 (m, 2H), 1.70–1.54 (m, 5H), 1.49–1.36 (m, 2 H), 1.20–1.27 (m, 4H); ¹³C NMR (500 MHz, CDCl₃): δ = 165.87, (C=O) 157.55 (C), 139.86 (C), 139.24 (CH), 136.53 (C), 119.50 (CH), 113.16 (CH₂), 111.20 (CH), 90.48 (C), 72.65 (CH₂), 48.92 (CH), 33.15 (CH₂), 25.54 (CH₂), 24.88 (CH₂), 19.48 (CH₃).

[4-Iodo-3-(2-methylallyloxy)phenyl]-(1-piperidyl)methanone (26 b)

Compound **25** (1.4 g, 4.4 mmol) was submitted to the same procedure described above for the preparation of **26 a**. The resulting oil was purified by column chromatography (silica gel, CH₂Cl₂). After concentration, 500 mg (30%) of a white solid was obtained; mp: 43 °C; ¹H NMR (500 MHz, CDCl₃): δ = 7.79 (d, *J* = 7.9 Hz, 1 H), 6.83 (d, *J* = 1.6 Hz, 1 H), 6.71 (dd, *J* = 7.9 Hz, 1.7 Hz, 1 H), 5.19 (s, 1H), 5.02 (s, 1H), 4.50 (s, 2 H), 3.69 (br s, 2 H), 3.33 (brs, 2H), 1.87 (s, 3 H), 1.68 (br s, 4 H), 1.51 (br s, 2H); ¹³C NMR (500 MHz, CDCl₃): δ = 169.27 (C=O), 157.28 (C), 139.86 (C), 139.37 (CH), 137.81(C), 120.57 (CH), 113.13 (CH₂), 110.78 (CH), 87.77 (C), 72.64 (CH₂), 24.56 (CH₂), 19.46 (CH₃).

3-Methyl-3-naphthalen-1-ylmethyl-2,3-dihydrobenzofuran-6-carboxylic acid cyclohexylamide (27)

Compound **26 a** (547 mg, 1.37 mmol) was submitted to the same procedure described above for the preparation of **11 a** using 1-naphthylboronic acid (282 mg, 1.64 mmol). Column chromatography (silica gel, heptane/EtOAc 8:2) afforded 368 mg (43 %) of the title compound as a colorless oil. ¹H NMR (300 MHz, CDCl₃): δ = 7.88–7.79 (m, 2 H), 7.75 (d, *J* = 8.2 Hz, 1 H), 7.47–7.31 (m, 3 H), 7.12–7.17 (m, 3 H), 6.84 (d, *J* = 8.0 Hz, 1 H), 5.85 (d, *J* = 7.8 Hz, 1 H), 4.57 (d, *J* = 8.8 Hz, 1 H), 4.09 (d, *J* = 8.8 Hz, 1 H), 3.96 (tdt, *J* = 12.2 Hz, 8.3 Hz, 4.0 Hz, 1 H), 3.44 (d, *J* = 13.9 Hz, 1H), 3.33 (d, *J* = 13.9 Hz, 1H), 2.02 (d, *J* = 13.1 Hz, 2 H), 1.82–1.61 (m, 3 H), 1.53–1.35 (m, 5H), 1.32–1.13 (m, 3 H); ¹³C NMR (500 MHz, CDCl₃): δ = 166.47 (C=O), 159.78 (C), 138.62 (C), 135.81 (C), 133.80 (C), 133.45 (C), 133.00 (C), 128.81 (CH), 128.72 (CH), 127.47 (CH), 125.75 (CH), 125.36 (CH), 124.97 (CH), 124.05 (CH), 123.42 (CH), 119.26 (CH), 108.33 (CH), 82.71 (CH₂), 48.60 (CH), 47.07 (CH₂), 41.40 (C), 33.22 (CH₂), 25.57 (CH₂), 24.87 (CH₂), 24.47(CH₃); HRMS (ES +) calcd for C₂₇H₂₉NO₂ [*M*+H]⁺ *m/z*: 400.2277, found: 400.2292.

(3-Methyl-3-naphthalen-1-ylmethyl-2,3-dihydrobenzofuran-6-yl)-piperidin-1-ylmethanone (28)

Compound **26 b** (528 mg, 1.37 mmol) was submitted to the same procedure described above for the preparation of **11 a** using 1-naphthylboronic acid (282 mg, 1.64 mmol). Column chromatography (silica gel, heptane/EtOAc 7:3) afforded 227 mg (43%) of the title compound as a colorless oil. ¹H NMR (500 MHz, CDCl₃): δ = 7.81 (dd, *J* = 8.1 Hz, 3.7 Hz, 2H), 7.75 (d, *J* = 8.2 Hz, 1H), 7.43–7.32 (m, 3H), 7.20 (d, *J* = 6.9 Hz, 1H), 6.80 (s, 1 H), 6.77–6.71 (m, 2H), 4.58 (d, *J* = 8.7 Hz, 1 H), 4.09 (d, *J* = 8.7 Hz, 1H), 3.68 (br s, 2 H), 3.47 (d, *J* = 13.9 Hz, 1H), 3.31 (m, 3H), 1.64–1.47 (m, 6 H), 1.43 (s, 3H); ¹³C NMR (500 MHz, CDCl₃): δ = 24.32 (CH₃), 24.64 (CH₂), 41.60 (CH₂), 46.94 (C), 82.84 (CH₂), 108.33 (CH), 119.02 (CH), 123.56 (CH), 124.19 (CH), 124.98 (CH), 125.27 (CH), 125.61 (CH), 127.46 (CH), 128.69 (CH), 128.77 (CH), 133.06 (C), 133.68 (C), 133.80 (C), 136.29 (C), 136.76 (C), 159.47 (C), 170.15 (C=O); HRMS (ES +) calcd for C₂₆H₂₇NO₂ [*M*+H]⁺ *m/z*: 386.2120, found: 386.2126.

(3-Methyl-3-naphthalen-2-ylmethyl-2,3-dihydrobenzofuran-6-yl)-piperidin-1-ylmethanone (29)

Compound **26 b** (528 mg, 1.37 mmol) was submitted to the same procedure described above for the preparation of **11 a** using 2-naphthylboronic acid (282 mg, 1.64 mmol). Column chromatography (silica gel, heptane/EtOAc 7:3) afforded 116 mg (22%) of the title compound as a colorless oil. ¹H NMR (500 MHz, CDCl₃): δ = 7.83–7.77 (m, 1 H), 7.72 (dd, *J* = 12.1 Hz, 6.1 Hz, 2H), 7.48–7.41 (m, 3H), 7.12 (dd, *J* = 8.4 Hz, 1.4 Hz, 1 H), 6.95 (d, *J* = 7.5 Hz, 1 H), 6.89 (dd, *J* = 7.5 Hz, 1.2 Hz, 1H), 6.75 (d, *J* = 0.7 Hz, 1H), 4.61 (d, *J* = 8.7 Hz, 1 H), 4.12 (d, *J* = 8.7 Hz, 1 H), 3.69 (s, 2 H), 3.33 (s, 2H), 3.06 (d, *J* = 13.4 Hz, 1H), 3.03 (d, *J* = 13.4 Hz, 1H), 1.58–1.67 (m, 6H), 1.41 (s, 3H); ¹³C NMR (500 MHz, CDCl₃): δ =

170.18 (C=O), 159.50 (C), 136.82 (C), 136.14 (C), 134.88 (C), 133.18 (C), 132.21 (C), 128.94 (CH), 128.79 (CH), 127.58 (CH), 127.57 (CH), 127.41 (CH), 125.99 (CH), 125.56 (CH), 123.51 (CH), 119.08 (CH), 108.24 (CH), 82.35 (CH₂), 46.75 (CH₂), 46.47 (C), 24.64 (CH₂), 24.59 (CH₃); HRMS (ES +) calcd for C₂₆H₂₇NO₂ [M+H]⁺ *m/z*: 386.2120, found: 386.2121.

[3-(4-Chlorobenzyl)-3-methyl-2,3-dihydrobenzofuran-6-yl]piperidin-1-ylmethanone (30)

Compound **26 b** (528 mg, 1.37 mmol) was submitted to the same procedure described above for the preparation of **11 a** using 4-chlorophenylboronic acid (256 mg, 1.64 mmol). Column chromatography (silica gel, heptane/EtOAc 6:4) afforded 187 mg (37 %) of the title compound as a colorless oil. ¹H NMR (500 MHz, CDCl₃): δ = 7.19 (d, *J* = 8.3 Hz, 2 H), 6.90 (dd, *J* = 6.1 Hz, 2.1 Hz, 4H), 6.74 (s, 1H), 4.48 (d, *J* = 8.8 Hz, 1H), 4.11 (d, *J* = 8.8 Hz, 1 H), 3.69 (br s, 2 H), 3.33 (br s, 2 H), 2.85 (d, *J* = 13.5 Hz, 1 H), 2.82 (d, *J* = 13.5 Hz, 1H), 1.66 (m, 6H), 1.36 (s, 3 H); ¹³C NMR (500 MHz, CDCl₃): δ = 170.08 (C=O), 159.47 (C), 136.92 (C), 135.67 (C), 135.58 (C), 132.58 (C), 131.60 (CH), 128.10 (CH), 123.44 (CH), 119.13 (CH), 108.28 (CH), 82.23 (CH), 46.17 (C), 46.01 (C), 24.62 (CH₂), 24.37 (CH₂); HRMS (ES +) calcd for C₂₂H₂₄ClNO₂ [M+H]⁺ *m/z*: 370.1574, found: 370.1596.

[3-[(4-Methoxyphenyl)methyl]-3-methyl-2,3-dihydrobenzofuran-6-yl]-(1-piperidyl)methanone (31)

Compound **26 b** (275 mg, 0.71 mmol) was submitted to the same procedure described above for the preparation of **11 a** using 4-methoxyphenylboronic acid (130 mg, 0.85 mmol). Column chromatography (silica gel, heptane/EtOAc 6:4) afforded 133 mg (51 %) of the title compound as a colorless oil. ¹H NMR (300 MHz, CDCl₃): δ = 6.94–6.85 (m, 4 H), 6.76 (dt, *J* = 4.8 Hz, 2.8 Hz, 2 H), 4.49 (t, *J* = 9.3 Hz, 1H), 4.08 (d, *J* = 8.7 Hz, 1 H), 3.73–3.61 (m, 2 H), 3.33 (s, 2 H), 2.83 (d, *J* = 13.5 Hz, 1 H), 2.78 (d, *J* = 13.5 Hz, 1 H), 1.75–1.44 (m, 6 H), 1.33 (s, 3H); ¹³C NMR (500 MHz, CDCl₃): δ = 170.66 (C=O), 159.87 (C), 158.73 (C), 136.99 (C), 136.68 (C), 131.70 (C), 129.70 (CH), 123.89 (CH), 119.46 (CH), 113.76 (CH), 108.53 (CH), 82.69 (CH₂), 55.60 (CH₃), 46.68 (C), 46.10 (CH₂), 25.02 (CH₂), 24.91 (CH₃); HRMS (ES +) calcd for C₂₃H₂₇NO₃ [M+H]⁺ *m/z*: 366.2069, found: 336.2075.

[3-Methyl-3-(4-pyridylmethyl)-2,3-dihydrobenzofuran-6-yl]-(1-piperidyl)methanone (32)

Compound **26 b** (528 mg, 1.37 mmol) was submitted to the same procedure described above for the preparation of **11 a** using 4-pyridineboronic acid (201 mg, 1.64 mmol). Column chromatography (silica gel, CH₂Cl₂/EtOH 9:1) afforded 133 mg (15%) of the title compound as an off-white solid; mp: 115°C; ¹H NMR (300 MHz, CDCl₃): δ = 8.45 (d, *J* = 5.0 Hz, 2 H), 6.99–6.83 (m, 5 H), 6.75 (s, 1H), 4.47 (d, *J* = 8.9 Hz, 1H), 4.12 (d, *J* = 8.9 Hz, 1H), 3.69 (br s, 2H), 3.33 (br s, 2H), 2.89 (d, *J* = 13.1 Hz, 1 H), 2.86 (d, *J* = 13.1 Hz, 1 H), 1.52–1.68 (m, 6 H), 1.40 (s, 3H); ¹³C NMR (500 MHz, CDCl₃): δ = 170.09 (C=O), 159.61 (C), 149.56 (CH), 146.29 (C), 137.37 (C), 135.21 (C), 125.73 (CH), 123.48 (CH), 119.41 (CH), 108.62 (CH), 82.30 (CH₂), 46.19 (C), 46.14 (CH₂), 24.76 (CH₂), 24.58 (CH₃); HRMS (ES +) calcd for C₂₁H₂₄N₂O₂ [M+H]⁺ *m/z*: 337.1916, found: 337.1902.

(S)-3-Benzyl-3-methyl-2,3-dihydrobenzofuran-6-carboxylic acid piperidine amide (33) and (R)-3-benzyl-3-methyl-2,3-dihydrobenzofuran-6-carboxylic acid piperidine amide (34)

Optimal analytical conditions for separation of the two enantiomers from racemic mixture **18** were determined using the following conditions: CYCLOBOND DMP column (Supelco Cat. No. 20724AST) 25 cm × 4.6 mm i.d., 5 μm, mobile phase: CH₃CN/AcOH/TEA 100:0.01:0.05, *T* = 10°C, flow rate: 0.3 mL min⁻¹, detection: UV (λ = 288 nm), injection volume: 10 μL, sample: 4.0 mg mL⁻¹ of compound **18** in solution (CH₃CN/AcOH/TEA 100:0.01:0.05); *t*_R for compound **33**: 15.73 min; *t*_R for compound **34**: 16.63 min.

A loading study revealed that up to 40 μg (10 μL of a 4.0 mg mL^{-1} solution in $\text{CH}_3\text{CN}/\text{AcOH}/\text{TEA}$ 100:0.01:0.05) could be loaded on an analytical CYCLOBOND DMP column while maintaining good resolution and selectivity. After translation of analytical loading conditions to the preparative scale, optimal conditions were obtained with the following parameters: CYCLOBOND DMP column (Supelco Cat. No. 20744AST) 25 cm \times 21.2 mm i.d., 5 μm , mobile phase: $\text{CH}_3\text{CN}/\text{AcOH}/\text{TEA}$ 100:0.01:0.05, $T = 10^\circ\text{C}$, flow rate: 6.4 mL min^{-1} , detection: UV ($\lambda = 288\text{ nm}$), injection volume: 80 μL , sample: 4.0 mg mL^{-1} of compound **18** in a solution of $\text{CH}_3\text{CN}/\text{AcOH}/\text{TEA}$ 100:0.01:0.05. Fractions for compounds **33** and **34** were collected separately. Fractions for each peak were concentrated to dryness by rotary evaporation at 40°C under vacuum. Fractions were then resuspended in CH_3CN and re-concentrated (3 \times in 25 mL CH_3CN) to remove residual moisture. Hexane was added to each flask to precipitate each enantiomer in the form of an off-white solid. The solid off-white powder resulting from each peak was scraped from the round-bottom flask, transferred to a vial, and left to air-dry overnight on a hot plate at low heat (30°C) to remove residual solvent. An enantiomeric purity analysis was then performed on each final product. Enantiomeric purity of compound **33** fell within acceptable limits ($>95\%$ *ee*); however, this was not the case with compound **34**. To ensure that sufficient material from compound **34** was produced, separation of additional racemic compound was re-initiated. The fractions from peak 2 were then collected, and sample recovery steps 2 and 3 were repeated. Because separations thus far produced peaks outside the acceptable limits of enantiomeric purity, the semi-pure compound **34** was re-purified on the preparatory system to remove residual compound **33** impurities. Sample recovery steps 2–4 were then repeated to obtain material with acceptable enantiomeric purity. Approximately 750 mg of racemic material was processed. Purity analysis indicated that the final solid material of compound **33** ($t_{\text{R}} = 16.84\text{ min}$) has an enantiomeric purity of 97.3 % while the final solid material of compound **34** ($t_{\text{R}} = 18.38\text{ min}$) has an enantiomeric purity of 97.5 %. A total of 109.4 mg of compound **33** was recovered; a total of 112.5 mg of compound **34** was recovered.

Supplementary Material

Refer to Web version on PubMed Central for supplementary material.

Acknowledgments

This work was supported in part by NIH Grant P30 M64023. We thank Dr. Kumar Kaluarachchi for performing NMR studies. The NMR facility at the M. D. Anderson Cancer Center is supported by Cancer Center Support Grant CA16672 awarded by the National Cancer Institute. We thank Ms. Beverly Parker for performing LC–MS and HRMS analyses.

References

1. McPartland JM. *Brain Res Rev.* 2004; 45:18–29. [PubMed: 15063097]
2. Ahn K, McKinney MK, Cravatt BF. *Chem Rev.* 2008; 108:1687–1707. [PubMed: 18429637]
3. Ehrhart J, Obregon D, Mori T, Hou H, Sun N, Bai Y, Klein T, Fernandez F, Tan J, Shytle RD. *J Neuroinflammation.* 2005; 2:29–41. [PubMed: 16343349]
4. Romero-Sandoval A, Eisenach JC. *Anesthesiology.* 2007; 106:787–794. [PubMed: 17413917]
5. Valenzano KJ, Tafesse L, Lee G, Harrison JE, Boulet JM, Gottshall SL, Mark L, Pearson MS, Miller W, Shan S, Rabadi L, Rotshteyn Y, Chaffer SM, Turchin PI, Elsemore DA, Toth M, Koetzner L, Whiteside GT. *Neuropharmacology.* 2005; 48:658–672. [PubMed: 15814101]
6. Yao BB, Hsieh GC, Frost JM, Fan Y, Garrison TR, Daza AV, Grayson GK, Zhu CZ, Pai M, Chandran P, Salyers AK, Wensink EJ, Honore P, Sullivan JP, Dart MJ, Meyer MD. *Br J Pharmacol.* 2008; 153:390–401. [PubMed: 17994110]
7. Naguib M, Diaz F, Xu J, Astruc-Diaz F, Craig S, Vivas-Mejia P, Brown DL. *Br J Pharmacol.* 2008; 155:1104–1116. [PubMed: 18846037]

8. Guindon J, Hohmann AG. *Br J Pharmacol*. 2008; 153:319–334. [PubMed: 17994113]
9. Karsak M, Gaffal E, Date R, Wang-Eckhardt L, Rehnelt J, Petrosino S, Starowicz K, Steuder R, Schlicker E, Cravatt B, Mechoulam R, Buettner R, Werner S, Di Marzo V, Tuting T, Zimmer A. *Science*. 2007; 316:1494–1497. [PubMed: 17556587]
10. Jhaveri MD, Richardson D, Kendall DA, Barrett DA, Chapman V. *J Neurosci*. 2006; 26:13318–13327. [PubMed: 17182782]
11. Matsuda LA, Lolait SJ, Brownstein MJ, Young AC, Bonner TI. *Nature*. 1990; 346:561–564. [PubMed: 2165569]
12. Munro S, Thomas KL, Abu-Shaar M. *Nature*. 1993; 365:61–65. [PubMed: 7689702]
13. Herkenham M, Lynn AB, Little MD, Johnson MR, Melvin LS, de Costa BR, Rice KC. *Proc Natl Acad Sci USA*. 1990; 87:1932–1936. [PubMed: 2308954]
14. Ameri A. *Prog Neurobiol*. 1999; 58:315–348. [PubMed: 10368032]
15. Facci L, Dal Toso R, Romanello S, Buriani A, Skaper SD, Leon A. *Proc Natl Acad Sci USA*. 1995; 92:3376–3380. [PubMed: 7724569]
16. Warms CA, Turner JA, Marshall HM, Cardenas DD. *Clin J Pain*. 2002; 18:154–163. [PubMed: 12048417]
17. Davis MP. *Support Care Cancer*. 2007; 15:363–372. [PubMed: 17131133]
18. Khaliq W, Alam S, Puri N. *Cochrane Database Syst Rev*. 2007; 2:CD004846. [PubMed: 17443559]
19. Tassone DM, Boyce E, Guyer J, Nuzum D. *Clin Ther*. 2007; 29:26–48. [PubMed: 17379045]
20. Gilron I, Coderre TJ. *Expert Opin Emerging Drugs*. 2007; 12:113–126.
21. Jensen MP, Chodroff MJ, Dworkin RH. *Neurology*. 2007; 68:1178–1182. [PubMed: 17420400]
22. Cox ML, Haller VL, Welch SP. *Eur J Pharmacol*. 2007; 570:50–56. [PubMed: 17588560]
23. Beltramo M, Bernardini N, Bertorelli R, Campanella M, Nicolussi E, Fredduzzi S, Reggiani A. *Eur J Neurosci*. 2006; 23:1530–1538. [PubMed: 16553616]
24. Ibrahim MM, Rude ML, Stagg NJ, Mata HP, Lai J, Vanderah TW, Porreca F, Buckley NE, Makriyannis A, Malan TP Jr. *Pain*. 2006; 122:36–42. [PubMed: 16563625]
25. Wotherspoon G, Fox A, McIntyre P, Colley S, Bevan S, Winter J. *Neuroscience*. 2005; 135:235–245. [PubMed: 16084654]
26. Zhang J, Hoffert C, Vu HK, Groblewski T, Ahmad S, O'Donnell D. *Eur J Neurosci*. 2003; 17:2750–2754. [PubMed: 12823482]
27. Walczak JS, Pichette V, Leblond F, Desbiens K, Beaulieu P. *Neuroscience*. 2005; 132:1093–1102. [PubMed: 15857713]
28. Walczak JS, Pichette V, Leblond F, Desbiens K, Beaulieu P. *J Neurosci Res*. 2006; 83:1310–1322. [PubMed: 16511871]
29. Page D, Yang H, Brown W, Walpole C, Fleurent M, Fyfe M, Gaudreault F, St-Onge S. *Bioorg Med Chem Lett*. 2007; 17:6183–6187. [PubMed: 17884494]
30. Giblin GMP, O'Shaughnessy CT, Naylor A, Mitchell WL, Eatheron AJ, Slingsby BP, Rawlings DA, Goldsmith P, Brown AJ, Haslam CP, Clayton NM, Wilson AW, Chessell IP, Wittington AR, Green R. *J Med Chem*. 2007; 50:2597–2600. [PubMed: 17477516]
31. Huffman JW. *Mini Rev Med Chem*. 2005; 5:641–649. [PubMed: 16026310]
32. Huffman JW, Yu S, Showalter V, Abood ME, Wiley JL, Compton DR, Martin BR, Bramblett RD, Reggio PH. *J Med Chem*. 1996; 39:3875–3877. [PubMed: 8831752]
33. Murineddu G, Lazzari P, Ruiu S, Sanna A, Loriga G, Manca I, Falzoi M, Dessi C, Curzu MM, Chelucci G, Pani L, Pinna GA. *J Med Chem*. 2006; 49:7502–7512. [PubMed: 17149879]
34. Manera C, Benetti V, Castelli MP, Cavallini T, Lazzarotti S, Pibiri F, Saccomanni G, Tuccinardi T, Vannacci A, Martinelli A, Ferrarini PL. *J Med Chem*. 2006; 49:5947–5957. [PubMed: 17004710]
35. Salo OMH, Raitio KH, Savinainen JR, Nevalainen T, Lahtela-Kakkonen M, Laitinen JT, J3rvinen T, Poso A. *J Med Chem*. 2005; 48:7166–7171. [PubMed: 16279774]
36. Ohta H, Ishizaka T, Yoshinaga M, Morita A, Tomishima Y, Toda Y, Saito S. *Bioorg Med Chem Lett*. 2007; 17:5133–5135. [PubMed: 17643986]

37. Ohta H, Ishizaka T, Tatsuzuki M, Yoshinaga M, Iida I, Tomishima Y, Toda Y, Saito S. *Bioorg Med Chem Lett*. 2007; 17:6299–6304. [PubMed: 17884496]
38. Brink CB. *Trends Pharmacol Sci*. 2002; 23:454. [PubMed: 12368066]
39. Kenakin T. *Trends Pharmacol Sci*. 1995; 16:256–258. [PubMed: 7482982]
40. Dziadulewicz EK, Bevan SJ, Brain CT, Coote PR, Culshaw AJ, Davis AJ, Edwards LJ, Fisher AJ, Fox AJ, Gentry C, Groarke A, Hart TW, Huber W, James IF, Kesingland A, LaVecchia L, Loong Y, Lyothier I, McNair K, O'Farrell C, Peacock M, Portmann R, Schopfer U, Yaqoob M, Zadrobilek J. *J Med Chem*. 2007; 50:3851–3856. [PubMed: 17630726]
41. Gardin A, Kucher K, Kiese B, Appel-Dingemanse S. *Drug Metab Dispos*. 2009; 37:827–833. [PubMed: 19144772]
42. Diaz P, Xu JJ, Astruc-Diaz F, Pan H-M, Brown DL, Naguib M. *J Med Chem*. 2008; 51:4932–4947. [PubMed: 18666769]
43. Yao BB, Hsieh G, Daza AV, Fan Y, Grayson GK, Garrison TR, El Kouhen O, Hooker BA, Pai M, Wensink EJ, Salyers AK, Chandran P, Zhu CZ, Zhong C, Ryther K, Gallagher ME, Chin C-L, Tovcimak AE, Hradil VP, Fox GB, Dart MJ, Honore P, Meyer MD. *J Pharmacol Exp Ther*. 2009; 328:141–151. [PubMed: 18931146]
44. McGaraughty S, Chu KL, Dart MJ, Yao BB, Meyer MD. *Neuroscience*. 2009; 158:1652–1661. [PubMed: 19063946]
45. Diaz P, Phatak SS, Xu J, Astruc-Diaz F, Cavasotto CN, Naguib M. *J Med Chem*. 2009; 52:433–444. [PubMed: 19115816]
46. Edgar KJ, Falling SN. *J Org Chem*. 1990; 55:5287–5291.
47. Diaz P, Gendre F, Stella L, Charpentier B. *Tetrahedron*. 1998; 54:4579–4590.
48. Szlosek-Pinaud M, Diaz P, Martinez J, Lamaty F. *Tetrahedron Lett*. 2003; 44:8657–8659.
49. Szlosek-Pinaud M, Diaz P, Martinez J, Lamaty F. *Tetrahedron*. 2007; 63:3340–3349.
50. Flack HD. *Acta Crystallogr*. 1983; A39:876–881.
51. Hoof RWW, Straver LH, Spek AL. *J Appl Crystallogr*. 2008; 41:96–103. [PubMed: 19461838]
52. Cheng J. *BMC Struct Biol*. 2008; 8:18–30. [PubMed: 18366648]
53. Hazai E, Bikadi Z. *J Struct Biol*. 2008; 162:63–74. [PubMed: 18249138]
54. Larsson P, Wallner B, Lindahl E, Elofsson A. *Protein Sci*. 2008; 17:990–1002. [PubMed: 18441233]
55. Cherezov V, Rosenbaum DM, Hanson MA, Rasmussen SG, Thian FS, Kobilka TS, Choi HJ, Kuhn P, Weis WI, Kobilka BK, Stevens RC. *Science*. 2007; 318:1258–1265. [PubMed: 17962520]
56. Rasmussen SG, Choi HJ, Rosenbaum DM, Kobilka TS, Thian FS, Edwards PC, Burghammer M, Ratnala VR, Sanishvili R, Fischetti RF, Schertler GF, Weis WI, Kobilka BK. *Nature*. 2007; 450:383–387. [PubMed: 17952055]
57. Rosenbaum DM, Cherezov V, Hanson MA, Rasmussen SG, Thian FS, Kobilka TS, Choi HJ, Yao XJ, Weis WI, Stevens RC, Kobilka BK. *Science*. 2007; 318:1266–1273. [PubMed: 17962519]
58. Bhattacharya S, Hall SE, Li H, Vaidehi N. *Biophys J*. 2008; 94:2027–2042. [PubMed: 18065472]
59. Niv MY, Skrabanek L, Filizola M, Weinstein H. *J Comput-Aided Mol Des*. 2006; 20:437–448. [PubMed: 17103019]
60. Pei Y, Mercier RW, Anday JK, Thakur GA, Zvonok AM, Hurst D, Reggio PH, Janero DR, Makriyannis A. *Chem Biol*. 2008; 15:1207–1219. [PubMed: 19022181]
61. Tikhonova IG, Best RB, Engel S, Gershengorn MC, Hummer G, Costanzi S. *J Am Chem Soc*. 2008; 130:10141–10149. [PubMed: 18620390]
62. Tuccinardi T, Ferrarini PL, Manera C, Ortore G, Saccomanni G, Martinelli A. *J Med Chem*. 2006; 49:984–994. [PubMed: 16451064]
63. Vilardaga JP. *Nat Chem Biol*. 2006; 2:395–396. [PubMed: 16850011]
64. Weis WI, Kobilka BK. *Curr Opin Struct Biol*. 2008; 18:734–740. [PubMed: 18957321]
65. Kobilka BK. *Biochim Biophys Acta*. 2007; 1768:794–807. [PubMed: 17188232]
66. Mirzadegan T, Benko G, Filipek S, Palczewski K. *Biochemistry*. 2003; 42:2759–2767. [PubMed: 12627940]
67. Xie XQ, Chen JZ, Billings EM. *Proteins Struct Funct Bioinf*. 2003; 53:307–319.

68. Ballesteros, JA.; Weinstein, H.; Stuart, CS. *Methods in Neurosciences*. Vol. 25. Academic Press; 1995. p. 366-428.
69. Sali A, Blundell TL. *J Mol Biol*. 1993; 234:779–815. [PubMed: 8254673]
70. Gouldson P, Calandra B, Legoux P, Kerneis A, Rinaldi-Carmona M, Barth F, Le Fur G, Ferrara P, Shire D. *Eur J Pharmacol*. 2000; 401:17–25. [PubMed: 10915832]
71. Montero C, Campillo NE, Goya P, Paez JA. *Eur J Med Chem*. 2005; 40:75–83. [PubMed: 15642412]
72. Tao Q, McAllister SD, Andreassi J, Nowell KW, Cabral GA, Hurst DP, Bachtel K, Ekman MC, Reggio PH, Abood ME. *Mol Pharmacol*. 1999; 55:605–613. [PubMed: 10051546]
73. Cavasotto CN, Orry AJ, Murgolo NJ, Czarniecki MF, Kocsi SA, Hawes BE, O'Neill KA, Hine H, Burton MS, Voigt JH, Abagyan RA, Bayne ML, Monsma FJ Jr. *J Med Chem*. 2008; 51:581–588. [PubMed: 18198821]
74. Cavasotto CN, Phatak SS. *Drug Discovery Today*. 2009; 14:676–683. [PubMed: 19422931]
75. Cavasotto CN, Kovacs JA, Abagyan RA. *J Am Chem Soc*. 2005; 127:9632–9640. [PubMed: 15984891]
76. Cavasotto CN, Liu G, James SY, Hobbs PD, Peterson VJ, Bhattacharya AA, Kolluri SK, Zhang XK, Leid M, Abagyan R, Liddington RC, Dawson MI. *J Med Chem*. 2004; 47:4360–4372. [PubMed: 15317450]
77. Kovacs JA, Cavasotto CN, Abagyan R. *J Comput Theo Nanosci*. 2005; 2:354–361.
78. Mukherjee S, Adams M, Whiteaker K, Daza A, Kage K, Cassar S, Meyer M, Yao BB. *Eur J Pharmacol*. 2004; 505:1–9. [PubMed: 15556131]
79. Polomano RC, Mannes AJ, Clark US, Bennett GJ. *Pain*. 2001; 94:293–304. [PubMed: 11731066]
80. Chaplan SR, Bach FW, Pogrel JW, Chung JM, Yaksh TL. *J Neurosci Methods*. 1994; 53:55–63. [PubMed: 7990513]
81. Dixon W. *J Am Stat Assoc*. 1965; 60:967–978.
82. Lipinski CA, Lombardo F, Dominy BW, Feeney PJ. *Adv Drug Delivery Rev*. 2001; 46:3–26.
83. Banker MJ, Clark TH, Williams JA. *J Pharm Sci*. 2003; 92:967–974. [PubMed: 12712416]
84. Gres MC, Julian B, Bourrie M, Meunier V, Roques C, Berger M, Boulenc X, Berger Y, Fabre G. *Pharm Res*. 1998; 15:726–733. [PubMed: 9619781]
85. Hunter J, Jepson MA, Tsuruo T, Simmons NL, Hirst BH. *J Biol Chem*. 1993; 268:14991–14997. [PubMed: 8100817]
86. Maron DM, Ames BN. *Mutat Res*. 1983; 113:173–215. [PubMed: 6341825]
87. Mathes C. *Expert Opin Ther Targets*. 2006; 10:319–327. [PubMed: 16548779]
88. Gouldson PR, Kidley NJ, Bywater RP, Psaroudakis G, Brooks HD, Diaz C, Shire D, Reynolds CA. *Proteins Struct Funct Bioinf*. 2004; 56:67–84.
89. Park JH, Scheerer P, Hofmann KP, Choe HW, Ernst OP. *Nature*. 2008; 454:183–187. [PubMed: 18563085]
90. Fernandez-Fuentes N, Rai BK, Madrid-Aliste CJ, Fajardo JE, Fiser A. *Bioinformatics*. 2007; 23:2558–2565. [PubMed: 17823132]
91. Read RJ, Chavali G. *Proteins Struct Funct Bioinf*. 2007; 69:27–37.
92. Ahuja S, Hornak V, Yan EC, Syrett N, Goncalves JA, Hirshfeld A, Ziliox M, Sakmar TP, Sheves M, Reeves PJ, Smith SO, Eilers M. *Nat Struct Mol Biol*. 2009; 16:168–175. [PubMed: 19182802]
93. Kobilka B, Schertler GF. *Trends Pharmacol Sci*. 2008; 29:79–83. [PubMed: 18194818]
94. Chin CN, Murphy JW, Huffman JW, Kendall DA. *J Pharmacol Exp Ther*. 1999; 291:837–844. [PubMed: 10525107]
95. Ashton JC, Wright JL, McPartland JM, Tyndall JD. *Curr Med Chem*. 2008; 15:1428–1443. [PubMed: 18537620]
96. Song ZH, Slowey CA, Hurst DP, Reggio PH. *Mol Pharmacol*. 1999; 56:834–840. [PubMed: 10496968]
97. McAllister SD, Tao Q, Barnett-Norris J, Buehner K, Hurst DP, Guarnieri F, Reggio PH, Nowell Harmon KW, Cabral GA, Abood ME. *Biochem Pharmacol*. 2002; 63:2121–2136. [PubMed: 12110371]

98. Poso A, Huffman JW. *Br J Pharmacol*. 2008; 153:335–346. [PubMed: 17982473]
99. Cavasotto CN, Abagyan RA. *J Mol Biol*. 2004; 337:209–225. [PubMed: 15001363]
100. Cavasotto CN, Orry AJ, Abagyan RA. *Proteins Struct Funct Bioinf*. 2003; 51:423–433.
101. Monti MC, Casapullo A, Cavasotto CN, Napolitano A, Riccio R. *ChemBioChem*. 2007; 8:1585–1591. [PubMed: 17691073]
102. Monti MC, Casapullo A, Cavasotto CN, Tosco A, Dal Piaz F, Ziemys A, Margarucci L, Riccio R. *Chemistry*. 2009; 15:1155–1163. [PubMed: 19065693]
103. Ibrahim MM, Deng H, Zvonok A, Cockayne DA, Kwan J, Mata HP, Vanderah TW, Lai J, Porreca F, Makriyannis A, Malan TP Jr. *Proc Natl Acad Sci USA*. 2003; 100:10529–10533. [PubMed: 12917492]
104. Ibrahim MM, Porreca F, Lai J, Albrecht PJ, Rice FL, Khodorova A, Davar G, Makriyannis A, Vanderah TW, Mata HP, Malan TP Jr. *Proc Natl Acad Sci USA*. 2005; 102:3093–3098. [PubMed: 15705714]
105. Malan TP Jr, Ibrahim MM, Deng H, Liu Q, Mata HP, Vanderah T, Porreca F, Makriyannis A. *Pain*. 2001; 93:239–245. [PubMed: 11514083]
106. Pace, JM.; Tietje, KR.; Dart, MJ.; Meyer, MD. 3-Cycloalkylcarbonylindoles as Cannabinoid Receptor Ligands and Their Preparation, Pharmaceutical Compositions and Use for Treatment of Pain. Patent WO. 2006069196. 2006.
107. Johnson, MR.; Melvin, LS. *Cannabinoids as Therapeutic Agents*. CRC Press; Boca Raton: 1986.
108. Ross RA, Brockie HC, Stevenson LA, Murphy VL, Templeton F, Makriyannis A, Pertwee RG. *Br J Pharmacol*. 1999; 126:665–672. [PubMed: 10188977]

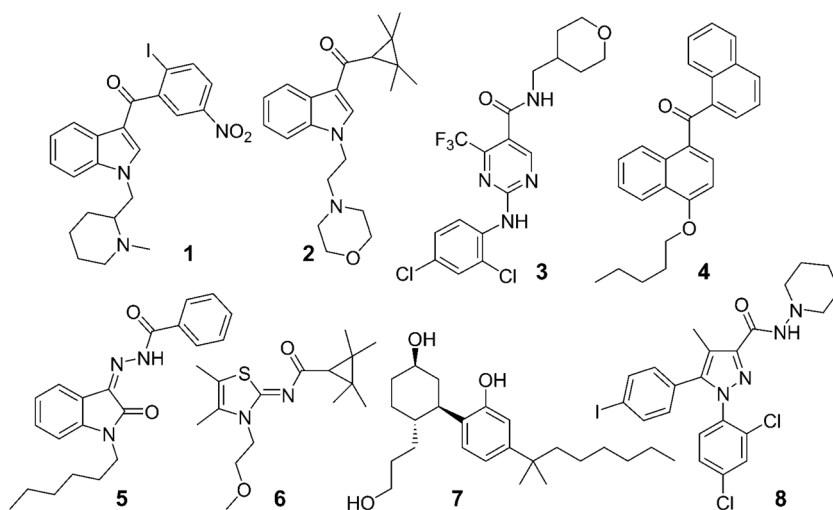


Figure 1. Structures of CB₂-selective modulators **1–6**, a nonselective CB agonist **7**, and a CB₁-selective antagonist **8**: **1** (AM1241),^[105] **2** (A-796260),^[106] **3** (GW842166X),^[30] **4** (CRA13),^[40] **5** (MDA19),^[42] **6** (A-83633),^[43] **7** (CP55,940),^[107] **8** (AM251).^[108]

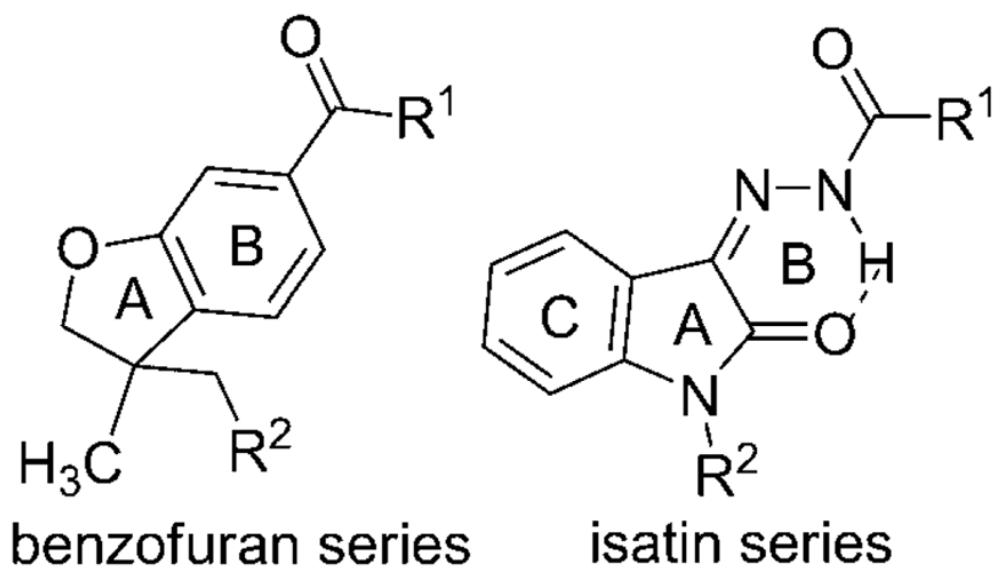


Figure 2.
Comparison of the 3,3-disubstituted-2,3-dihydro-1-benzofuran scaffold with the isatin scaffold.

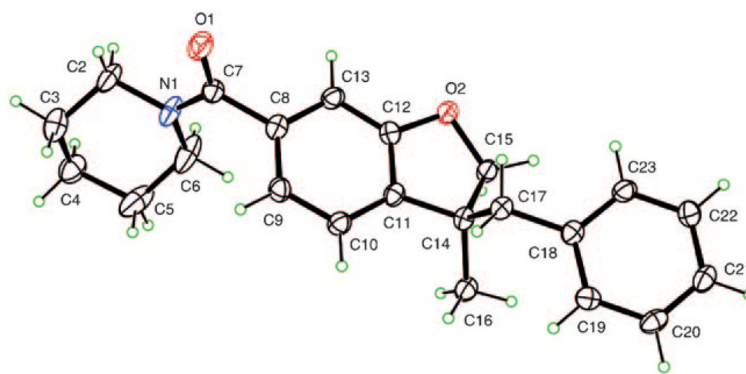


Figure 3.
Compound **33** with atom labeling shown.

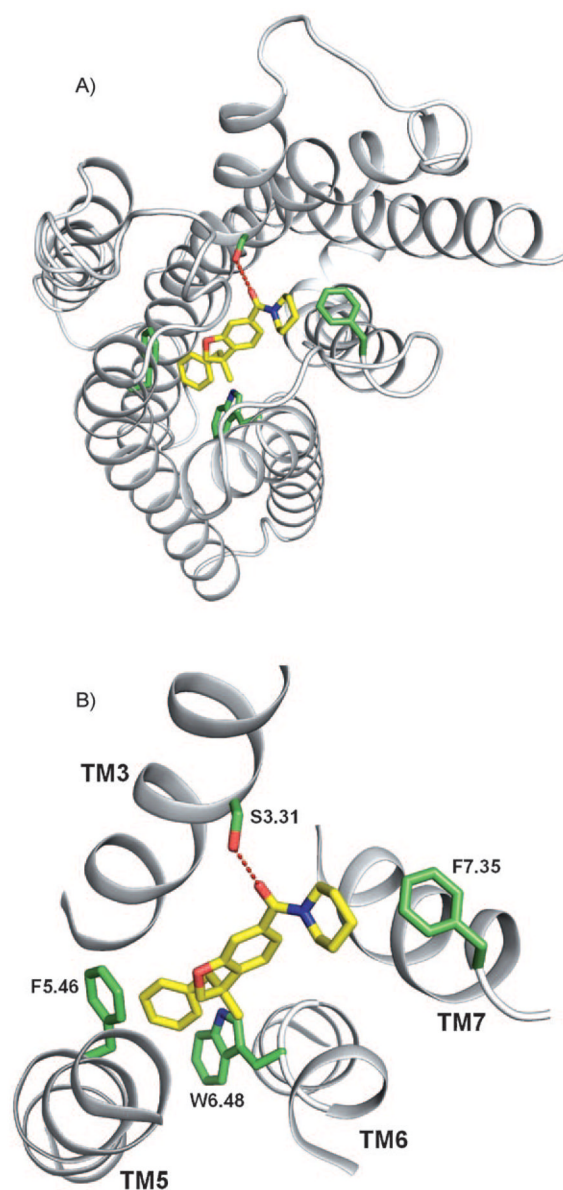


Figure 4.
A) CB₂ complexed with compound **33** (yellow carbon atoms). Transmembrane regions (TM) are shown as white ribbons; the image was prepared using PyMOL (<http://www.pymol.org>). B) A putative hydrogen bond between S3.31 and compound **33** (yellow carbon atoms) is represented as red dashes. The aromatic pocket is enclosed by residues F5.46 and W6.48 (green carbon atoms).

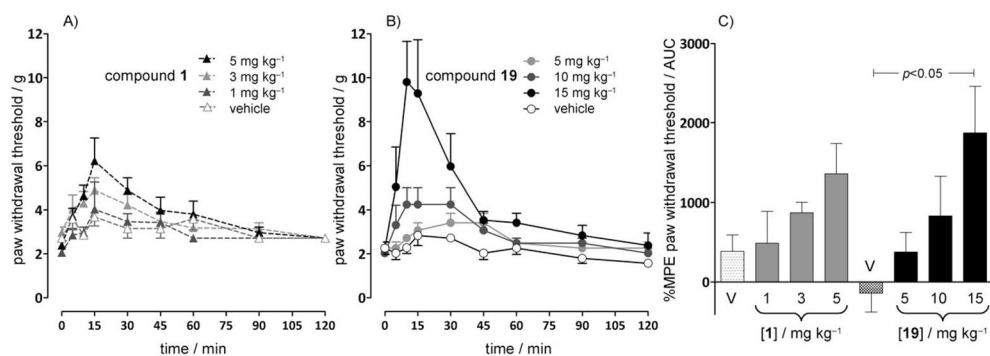
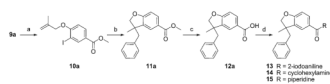
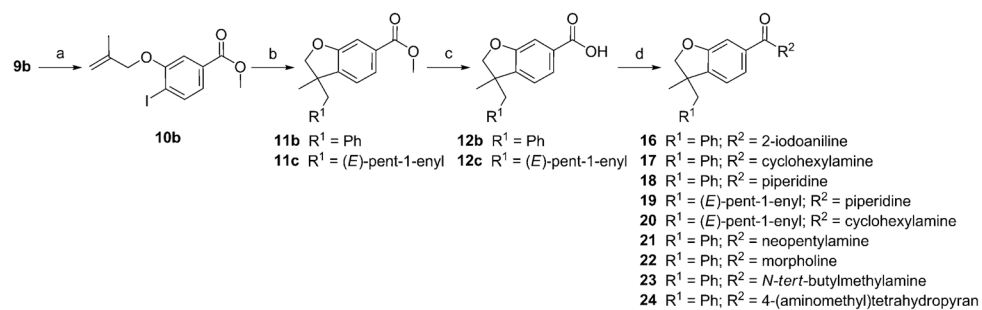


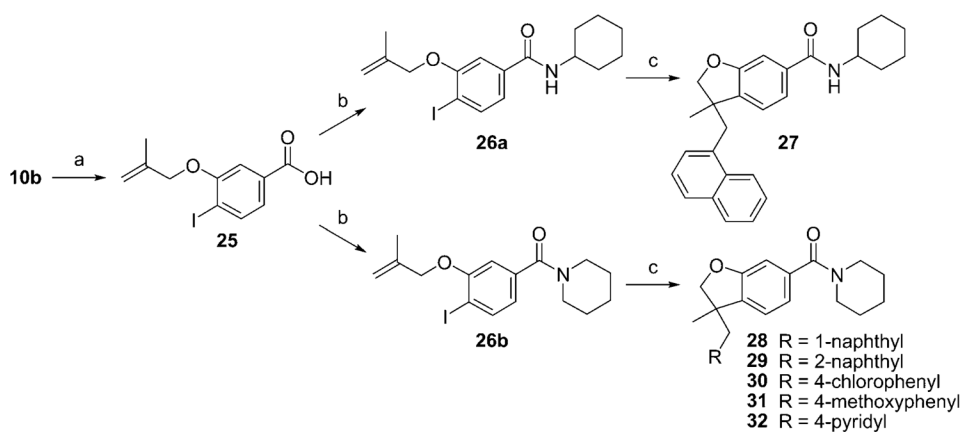
Figure 5. Effects of A) compound **1** and B) compound **19** administered by intraperitoneal injection on tactile allodynia in a paclitaxel-induced neuropathic pain model in rats ($n = 5-6$ per group). C) Compound **19** dose-dependently attenuated tactile allodynia in this model, as evidenced by an increase in the percent MPE withdrawal threshold area under the curve (AUC); $P < 0.05$ between the vehicle (V) and compound **19** at 15 mg kg^{-1} (ANOVA followed by Tukey–Kramer test for multiple group comparison). Compound **1** did not affect the paw withdrawal threshold. The effects of compound **1**, a CB₂ ligand,^[103] at 1, 3, and 5 mg kg^{-1} were not significantly different from the effects induced by the vehicle.

**Scheme 1.**

Reagents and conditions: a) K_2CO_3 , methyl ethyl ketone, 3-bromo-2-methylpropene; b) K_2CO_3 , $[Pd(OAc)_2]$, nBu_4NCl , DMF, $PhB(OH)_2$; c) $NaOH$, EtOH, THF, H_2O ; d) HATU, DiPEA, DMF, CH_2Cl_2 , 2-iodoaniline for **13** or cyclohexylamine for **14** or piperidine for **15**.

**Scheme 2.**

Reagents and conditions: a) K₂CO₃, methyl ethyl ketone, 3-bromo-2-methylpropene; b) K₂CO₃, [Pd(OAc)₂], *n*Bu₄NCl, DMF, PhB(OH)₂ for **11 b** or 1-penten-1-ylboronic acid for **11 c**; c) NaOH, EtOH, THF, H₂O; d) HATU, DiPEA, DMF, CH₂Cl₂, 2-iodoaniline for **16** or cyclohexylamine for **17** and **20** or piperidine for **18** and **19** or neopentylamine for **21** or morpholine for **22** or *N*-*tert*-butylmethylamine for **23** or 4-(aminomethyl)tetrahydropyran for **24**.

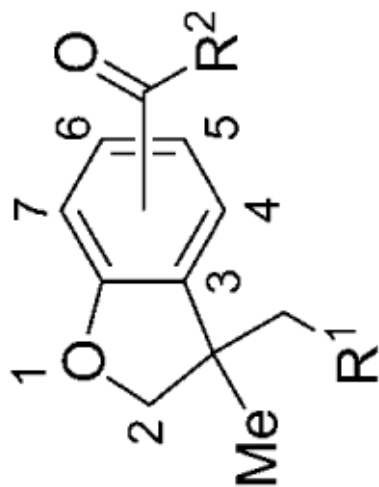
**Scheme 3.**

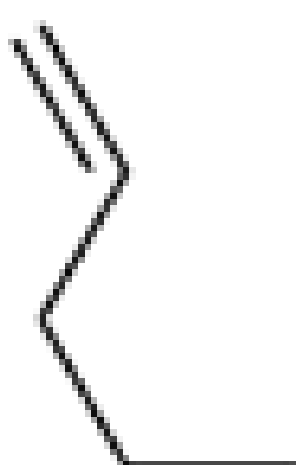
Reagents and conditions: a) NaOH, EtOH, THF, H₂O; b) HATU, DiPEA, DMF, CH₂Cl₂, cyclohexylamine for **26 a** or piperidine for **26 b**; c) K₂CO₃, [Pd(OAc)₂], *n*Bu₄NCl, DMF, 1-naphthylboronic acid for **27** and **28** or 2-naphthylboronic acid for **29** or 4-chlorophenylboronic acid for **30** or 4-methoxyboronic acid for **31** or 4-pyridylboronic acid for **32**.

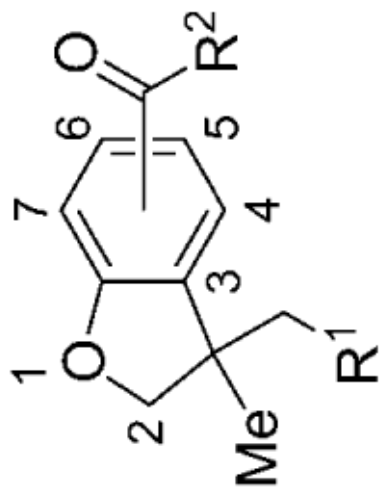
Table 1

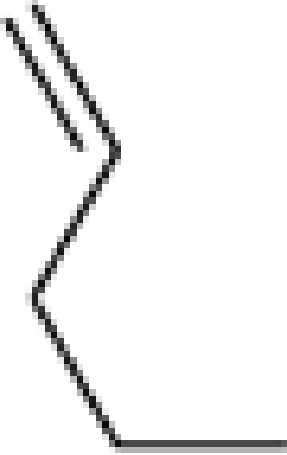
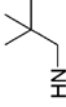
Potency (EC_{50}) and maximal stimulation (E_{max})s of hCB₁ and hCB₂ by compounds **13**–**32**.^[a]

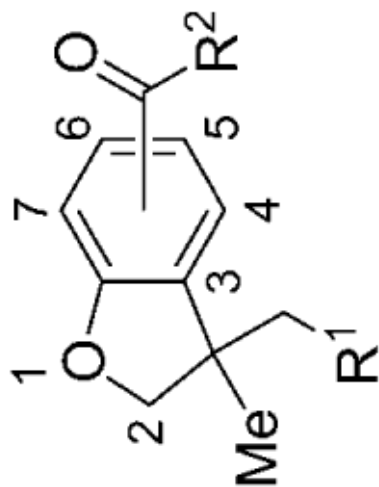
Compound	R ¹	R ²	R ² position	γ-[³⁵ S]GTP hCB ₁		γ-[³⁵ S]GTP hCB ₂	
				EC ₅₀ [nm ± SEM]	E _{max} [%][b]	EC ₅₀ [nm ± SEM]	E _{max} [%][b]
13	phenyl	N-(2-iodophenyl)	5	>10 000	ND[c]	>10 000	ND
14	phenyl	N-cyclohexyl	5	>10 000	ND	406 ± 1.4	47.1
15	phenyl	1-piperidyl	5	>10 000	ND	>10 000	ND
16	phenyl	N-(2-iodophenyl)	6	>10 000	ND	>10 000	ND
17	phenyl	N-cyclohexyl	6	>10 000	ND	478 ± 1.3	54.3
18	phenyl	1-piperidyl	6	>10 000	ND	128 ± 32	88.3
33		S enantiomer (1) of 18	6	>10 000	ND	108.02	86
34		R enantiomer (2) of 18	6	>10 000	ND	960.89	43.3

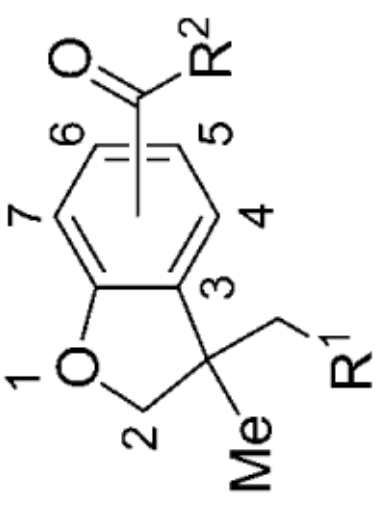
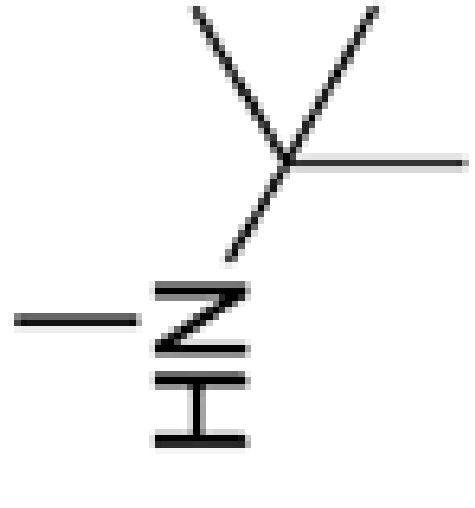


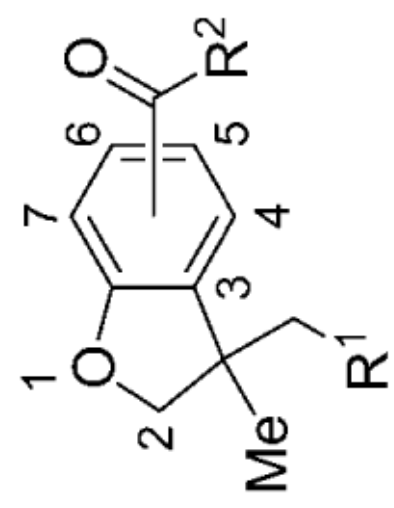
Compound	R ¹	R ²	γ-[³⁵ S]GTP hCB ₁		γ-[³⁵ S]GTP hCB ₂	
			EC ₅₀ [nM] ± SEM]	E _{max} [%][b]	EC ₅₀ [nM] ± SEM]	E _{max} [%][b]
19		1-piperidyl	856 ± 1.2	60	48.9 ± 1.4	97.1

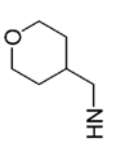


Compound	R ¹	R ²	γ-[³⁵ S]GTP hCB ₁		γ-[³⁵ S]GTP hCB ₂	
			EC ₅₀ [nM] ± SEM]	E _{max} [%][b]	EC ₅₀ [nM] ± SEM]	E _{max} [%][b]
20		N-cyclohexyl	>10 000	ND	839 ± 5.5	105
21	phenyl		>10 000	ND	246 ± 1.3	48.7
22	phenyl	morpholine	>10 000	ND	5583 ± 4.4	93



Compound	R ¹	R ²	γ-[³⁵ S]GTP hCB ₁		γ-[³⁵ S]GTP hCB ₂	
			EC ₅₀ [nm ± SEM]	E _{max} [%][b]	EC ₅₀ [nm ± SEM]	E _{max} [%][b]
	phenyl		2580 ± 1.5	ND	95.3 ± 1.8	91
						



Compound	R ¹	R ²	γ-[³⁵ S]GTP hCB ₁		γ-[³⁵ S]GTP hCB ₂	
			EC ₅₀ [nm ± SEM]	E _{max} [%] ^[a]	EC ₅₀ [nm ± SEM]	E _{max} [%] ^[a]
24	phenyl		>10 000	ND	659 ± 1.4	49
27	1-naphthyl	<i>N</i> -cyclohexyl	>10 000	ND	>10 000	ND
28	1-naphthyl	1-piperidyl	>10 000	ND	>10 000	ND
29	2-naphthyl	1-piperidyl	>10 000	ND	875 ± 1.4	112
30	4-chlorophenyl	1-piperidyl	1363 ± 1.4	86.9	56.2 ± 1.2	102
31	4-methoxyphenyl	1-piperidyl	>10 000	ND	234.68	77.1
32	4-pyridine	1-piperidyl	>10 000	ND	2801.44	62.5

ChemMedChem. Author manuscript; available in PMC 2012 January 21.

^[a] CB₁ and CB₂ assay data are presented as the mean of two determinations; reproducibility was monitored by the use of compound 7 as reference. For replicate determinations, the maximum variability tolerated in the test was ±20 % around the average of the replicates.

^[b] Efficacies for CB₁ or CB₂ are expressed as percentage relative to the efficacy of compound 7.

^[c] ND = not determined (plateau was not reached at a dose of 10 μm).

Table 2

Radioligand competitive binding assay data.

Ligand	K_i [nM] ^[a]	
	hCB ₁	hCB ₂
18	>10 000	422 ± 123
19	ND ^[b]	83.6 ± 23.8
20	>1000	>1000
29	430 ± 39	490 ± 45
30	ND	123 ± 16.5
7	3.4	1.8 ± 1.1
8	1.16 ± 0.01	ND

^[a]Values represent the mean ±SEM.^[b]ND = not determined.

Table 3ADMET profile for compound **18**.

Parameter	Value
Aqueous solubility (PBS, pH 7.4) at 2.0×10^{-4} M:	$31.8 \pm 1.8 \mu\text{M}$
Protein bound (human):	$82.8 \pm 11.1 \%$
Protein recovery (human):	$95.6 \pm 13.6 \%$
A-B permeability (TC7, pH 6.5/7.4) [10^{-6} cm s ⁻¹]:	52.2 ± 1.7
A-B permeability (% recovery):	$63.5 \pm 6.5 \%$
B-A permeability (TC7, pH 6.5/7.4) [10^{-6} cm s ⁻¹]:	16.2 ± 0.2
B-A permeability (% recovery):	$85.5 \pm 0.5 \%$
Ames test (strain TA98):	<0
Ames test (strain TA98 +S9):	<0
K ⁺ channel hERG automated patch-clamp (cardiac toxicity):	inactive at 1 μM